SEQUENCE STRATIGRAPHY OF MIOCENE SEQUENCES Kw2a AND m5.4, NEW JERSEY: ONSHORE TO OFFSHORE CORRELATIONS

by

TURAN ISCIMEN

A Thesis submitted to the

Graduate School–New Brunswick

Rutgers, The State University of New Jersey

For the degree of

Master of Science

Graduate Program in Geological Sciences

Written under the direction of

Dr. Kenneth G. Miller

And approved by

____

____

____

New Brunswick, New Jersey

JANUARY, 2014

ABSTRACT OF THE THESIS

Sequence Stratigraphy Of Miocene Sequences Kw2a And m5.4, New Jersey:

Onshore To Offshore Correlations

by

TURAN ISCIMEN

Thesis Director:

Dr. Kenneth G. Miller

I evaluated the upper lower Miocene Kw2a sequence in onshore New Jersey coastal plain coreholes and nearshore wells and its relationship to composite sequence m5.4 on the New Jersey continental shelf. I used Ocean Drilling Program Leg 174AX Cape May Zoo (CMZ) and Ocean View (OV) corehole and well log data to construct the anatomy of composite Kw2a sequence by integrating lithologic changes, grain size data, gamma ray logs, and benthic foraminiferal biofacies and paleodepths in a sequence stratigraphic framework. I identified 3 higher order sequences (Kw2a1, Kw2a2, and Kw2a3) and stratal boundaries (transgressive surfaces [TS] and maximum flooding surfaces [MFS]) within the composite Kw2a sequence. A thin, deepening upward LST is tentatively identified only at the base of the Kw2a1 higher order sequence at both sites.

Mud dominant, deepening and fining upward TST's are found in all 3 higher order sequences. MFS are associated with mud and *Uvigerina* spp. peaks and are overlain by, sandy coarsening and shallowing upward HST's. To test the physical correlation between onshore-nearshore and middle shelf systems, I identified Kw2a and higher order sequences in other ODP Leg 150A, 174AX, and U.S.G.S onshore and nearshore wells using gamma ray logs. I correlated gamma ray logs of the composite Kw2a sequence to onshore [Atlantic City (AC)] and nearshore wells (ACOW-1, 2, AMCOR-6011) and traced the Kw2a sequence on seismic profiles crossing these sites. I projected other onshore cores and logs to nearby seismic profiles. I traced the composite Kw2a sequence on seismic profiles directly to IODP Expedition 313 coreholes where I demonstrate that the composite Kw2a sequence is physically equivalent to composite m5.4 sequence.

DEDICATION

Sevgili Anne ve Babama

To My Beloved Mom and Dad

ACKNOWLEDGEMENT

I would like to express my very great appreciation to my principal advisor **Dr. Kenneth G. Miller** for his valuable and constructive contributions during the planning and development of this thesis and his great efforts to explain things as clearly and simply as possible. I consider that it is my privilege to work under his supervision. His willingness to give his time, and guidance has been very much appreciated.

I would also like to express my deep and sincere gratitude to my committee member **Dr. James V. Browning** for his valuable recommendations, comments, and his limitless time whenever I asked.

I am thankful to my other committee member **Dr. Donald Monteverde** for his support, encouragement and providing me data whenever I need.

I wish to acknowledge the help provided by **Dr. Gregory Mountain** in the well log and seismic analysis part of this thesis.

I am thankful to the **Turkish Petroleum Corporation** for providing me the opportunity of studying in graduate school in the U.S.

I would like to thank **faculty and staff of Department of Earth and Planetary Sciences** for creating a pleasant working environment, scientific atmosphere with their kindness, knowledge, and support.

I would like to thank **fellow graduate students** for their friendship, support and sharing the funniest and the toughest times always with their kindest company. I am particularly grateful to **Ms. Tuce Degirmenci**, **Mrs. Selen Esmeray Senlet**, **Ms. Masha Makarova**, and **Mr. Cesar Sequeira** for helping me accomplishing this study with their memorable fellowship and friendship.

It is inevitable to express my deep gratitude to **Ms. Buse Ceren Sengul** for her valuable support, patience, very special friendship, and her precious intimacy over thousand miles away.

I wish to thank my mother **Mrs. Yasemin Iscimen** and father **Mr. Mustafa Servet Iscimen** for providing me their countless support, courage, patience, understanding and great love from the beginning of my U.S. journey. I am thankful, humble and honored for being their only one son and I hope I have made them proud with me.

Last but not the least, I would like to appreciate any legendary scientists, specifically earth scientist, artists, politicians, and sportsmen, who have inspired the young generation and contributed to society and humanity by showing the honest, and legitimate way of usage of human power and taken their occupations even further. For, that matter, I wish to express my gratefulness personally to **Mr. Roger Federer** who has inspired me to be able to focus, work diligently, consistently and showed how not to give up until achieving a particular goal.

TABLE OF CONTENTS

ABSTRACT OF THE THESIS ii

DEDICATION iv

ACKNOWLEDGEMENT v

1 Introduction 1

2 Methods 6

2.1 Lithology, Lithofacies, and Paleodepositional Interpretation 6

2.2 Gamma Ray Log Interpretation 8

2.3 Benthic Foraminiferal Biofacies Paleodepth Distribution 8

2.4 Onshore-Offshore Well Log Projections and Seismic Correlation..... 12

3 Results 15

3.1 Cape May Zoo Corehole Interpretation 15

3.2 Ocean View Corehole Interpretation 22

3.3 Seismic Interpretation and Gamma Ray Log Correlation.................. 29

4 Discussion 34

5 Conclusion 39

6 References 43

7 Figures 52

8 Tables 74

LIST OF FIGURES

Figure 1: Generalized location map of New Jersey Transect (Miller et al., 2013a) 52

Figure 2: Sequence boundaries (Late Oligocene to Pleistocene) of offshore New Jersey at Expedition 313 Site (Miller et al., 2013a) 53

Figure 3: Generalized sequence stratigraphy of a clinoform (modified from Miller et al., 2013a) 54

Figure 4: Well log locations and figure numbers of seismic profiles in this study 55

Figure 5: Uninterpreted (above) and interpreted (below) seismic profiles of CH0698 5 and 9 seismic profiles show uniform thickness and gradient change over inner shelf. The calculation is provided in Table 2. 56

Figure 6: Integration of lithology, gamma ray log character, grain size, and semi quantitative benthic foraminifera paleobathymetrical curve of Cape May Zoo composite Kw2a sequence corehole data in a sequence stratigraphic framework ... 57

Figure 7: The proposed LST of higher order Kw2a1 sequence of Cape May Zoo corehole including stratal surfaces (SB, FS, and TS) and system tracts................................. 58

Figure 8: Grain size analysis of higher order Kw2a2 sequence in Cape May Zoo corehole shows MFS. Black arrows are showing fining direction. 59

Figure 9: The merged sequence boundary and transgressive surface that separates higher order sequence of Kw2a2 from Kw2a3 at 531.2 ft in Cape May Zoo corehole. 60

Figure 10: Integration of lithology, gamma ray log character, grain size, and semi quantitative benthic foraminifera paleobathymetrical curve of Ocean View composite Kw2a sequence corehole data in a paleodepositional and sequence stratigraphic framework 61

Figure 11: At 627 ft pale light gray indurated calcareous claystone marks the boundary between dark colored laminated shoreface-offshore transitional (inner neritic) mudstone and offshore, inner to middle neritic transgressive system tract facies of higher order Kw2a1 sequence in Ocean View corehole. 62

Figure 12: In Ocean View corehole, MFS marks the boundary between finely laminated inner neritic mud dominated TST facies and shelly, blocky fine to medium sand dominated HST facies. A flooding surface occurs within HST............................... 63

Figure 13: Gamma ray log correlation over Leg 150X, 174AX onshore well logs and U.S.G.S. onshore and offshore well logs regardless of seismic data. Higher order sequences Kw2a1, Kw2a2, and Kw2a3 were interpreted in CMZ, SIC, OV, AC, and ACOW1. 64

Figure 14: Loop correlation over CH0698 27, 38, 9, and 16 seismic profiles shows the continuity of Kw2a gamma ray log characters and equivalent seismic reflection of top and basal composite Kw2a sequence boundaries. 65

Figure 15: Gamma ray log correlation is projected onto CH0698 42 seismic profile and the sequence boundaries that traced from CH0698 38 seismic profile were loop correlated with previously proposed gamma ray log data peaks for top and basal sequence boundaries for composite Kw2a sequence. 66

Figure 16: Cape May Zoo gamma ray log data directly projected onto CH0698 42 line. Seismic reflections represent top and basal sequence boundaries of composite Kw2a sequence traced from OV, SIC, and Strathmere well logs. 67

Figure 17: Cape May gamma ray log data directly projected onto CH0698 42 line. Seismic reflections represent top and basal sequence boundaries of composite Kw2a sequence. 68

Figure 18: Younger strata onlap onto the upper sequence boundary of composite Kw2a sequence. An erosional relief, which is in connection with the overlying sequence boundary, is filled with younger (upper sequence) sediment 69

Figure 19: Loop correlated profile shows the physical connection between inner ACOW2 and middle shelf M27, M28, and M29 well logs in 4 different seismic profiles. The red colored reflection shows physical connection of onshore Kw2a sequence boundaries and m5.4 and m5.2 of sensu (Monteverde et al., 2008; and Miller et al., 2013a). 70

Figure 20: The red colored reflections show offshore equivalents of top and basal sequence boundaries of composite Kw2a sequence traced from CH0698 38 seismic profile to Oc270 529 seismic profile. (A closer view of Oc270 529 part of fig. 19) 71

Figure 21: The orange reflections show top and base of Kw2a composite sequence. Red colored reflections are gathered from Miller et al. (2013a). Upper sequence boundary of Kw2a seems to merge with m5.3 reflection at the landward side of M27, where seismic ambiguity occurs due to truncated m5.3 reflectionand continuonus tracing might lead to m5.2 reflection. 72

Figure 22: Comparison of Expedition 313 coreholes (M27, M28, and M29) ages Browning et al. (2013), Cape May Zoo and Ocean View coreholes Sr-isotope age data Kominz et al. (unpublished) and $\delta^{18}O$ data comparison with Mi events. Mi1b

and Mi2 events mark the sequence boundaries for onshore Kw2a and offshore m5.4 composite sequences. 73

LIST OF TABLES

Table 1: The original well log thicknesses are compared with the thicknesses of sequences after application of T-D chart and displayed on seismic profiles. This table also provides minimum distance between well log and nearest seismic profile and vertical dipline gradient for individual wells. 74

Table 2: The gradient and thickening estimation, are shown on this table with providing TWTT (two way travel time) and lateral traced distances individually on CH0698 5 and 9 seismic profiles. Overall average is estimated by taking mean of the two different estimations.. 75

Table 3: Sample data of CMZ corehole composite Kw2a sequence and benthic and planktonic foramifera numarical values are provided... 76

Table 4: CMZ corehole first five predominant benthic foraminiferal biofacies are provided with numerical values and relative precentages for each sample. 77

Table 5: Sample data of OV corehole composite Kw2a sequence, benthic and planktonic foramifera numarical values are provided. 78

Table 6: OV corehole first five predominant benthic foraminiferal biofacies are provided with numerical values and relative precentages for each sample 79

1 Introduction

Sequence stratigraphy is a multidisciplinary approach used to subdivide the sedimentary record using genetic criteria (Mitchum et al., 1977). Unconformity bounded sedimentary units, known as sequences (Mitchum et al., 1977), are identified and subdivided using important stratal surfaces, including sequence boundaries (SB), transgressive surfaces (TS), and flooding surfaces, especially the maximum flooding surface (MFS). These stratal surfaces represent changes in lithofacies, paleodepth, and depositional regime, are recognized using sedimentary facies stacking patterns, and are used to internally divide sequences into system tracts (Brown and Fisher, 1977; Catuneanu, 2006). System tracts are determined from outcrop, corehole, well log data, and seismic profiles that are integrated to interpret sequences at a variety of scales from small (10's of m) to large (10's of km) (Vail and Wornardt, 1990). The sequence stratigraphic method has been widely used in industry for hydrocarbon, coal, and mineral exploration and in academia to understand the nature of sedimentary basin fills (Catuneanu, 2006).

The sequence stratigraphy of the New Jersey shelf has attracted both academic and industry scientists. Initial seismic and corehole studies and surveys [Atlantic Margin Coring Project (AMCOR), Atlantic City Coring Well (ACOW)] by the U.S.G.S. (e.g., Poppe et al., 1976; Hathaway et al., 1979; Schlee, 1980; Poag, 1985) were followed by industry surveys (e.g. Greenlee et al., 1988; 1992). Commercial exploration studies targeted Mesozoic successions beneath the modern outer shelf and slope, but concluded hydrocarbon production there would be uneconomic. Onshore, coastal plain drilling

(Ocean Drilling Program (ODP) Legs 150X and 174AX) and offshore, continental shelf-slope drilling (ODP Legs 150, 174A, and Integrated Ocean Drilling Program (IODP) Expedition 313) provided core, well log, and seismic data targeting mostly Oligocene-Miocene sequences.

The New Jersey passive continental margin (Fig. 1) is an excellent location to study the stratigraphic record using sequence stratigraphic principles. New Jersey has been a passive continental margin from the Cretaceous through the Cenozoic and coastal plain and shelf tectonics have been dominated by simple thermo-flexural subsidence and sediment loading since rifting (Watts and Thorne, 1984; Kominz et al., 2008), though the effects of Glacial Isostatic Adjustment (Peltier, 1998) on the younger record and mantle dynamics (e.g., Rowley et al., 2013) on the longer record must be considered. There is an extensive database of seismic profiles, well log and corehole data available. Lithological variations in these neritic environments allow resolution of water depth changes because shallow water depositional strata laterally grade into one another in short distances compared to bathyal and abyssal depths (e.g., Van Morkhoven et al., 1986). In addition, neritic strata contain benthic foraminifera that can be used to reconstruct paleobathymetric changes. Benthic foraminifera biofacies provide relatively high paleobathymetric resolution (within 10's of meter scale) for paleodepths shallower than outer neritic (100 m) (e.g., Van Morkhoven et al., 1986).

The lower to middle Miocene NJ record consists of thick (hundreds of meters per sequence) Miocene sequences that have been seismically imaged under the inner to middle shelf (Poag, 1977; Monteverde et al., 2008). Previous studies (e.g. Miller et al., 1997, 2001, 2005; Browning et al., 2006; Monteverde et al., 2008; Mountain and Proust,

2010) have focused on stacking patterns, sea level changes, and large-scale seismic correlations of upper Oligocene to upper Miocene sequences. The correlation between the timing of $\delta^{18}O$ increases with sequence boundaries suggests a primary control on the development of the stratigraphic record has been eustatic change (Wright and Miller, 1992; Miller et al., 1996, 1998; Browning et al., 2013).

Sugarman et al. (1993) and Miller et al. (1997) studied onshore Miocene sequences in New Jersey and Monteverde et al. (2000, 2008) and Miller et al. (2013a) studied the Miocene seismic sequences on the New Jersey shelf. Although onshore Miocene sequences have been documented in detail and dated with ±1 m.y. resolution (e.g. Miller et al., 1997, 2002), they have only been provisionally correlated with offshore Miocene sequences using seismic profiles (Monteverde et al., 2008; Monteverde, 2008). Expedition 313 drilling on the inner-middle continental shelf (Fig. 1) provides a new impetus to reevaluate onshore to offshore correlations using seismic profiles. Expedition 313 linked seismic sequences (Monteverde et al., 2008; Monteverde, 2008) with cores and logs (Mountain et al., 2010; Miller et al., 2013 a, b). It also provided excellent age control (from ±0.25 to ±0.5 m.y.) on lower to middle Miocene sequences (Browning et al., 2013) that allows further evaluating onshore to offshore correlations using age control afforded by biostratigraphy and Sr-isotope stratigraphy.

Offshore sequence m5.4 is particularly interesting because integrated seismic profiles and core data suggest it is a composite of three higher order sequences (Miller et al., 2013a) (Fig. 2). Similarly, onshore sequence Kw2a appears to be a composite sequence (de Verteuil et al., 1997; Miller et al., 2001, 2005). Higher frequency base level changes create spatially limited, and temporally short (< 1 m.y.) higher order sequences.

A composite sequence is a lower order (typically 1 m.y. or 10 m.y. scale) sequence comprised of two or more higher order sequences that stack together to yield a pattern identifiable as sequence (Neal and Abreu, 2009). Higher order sequences may form either in LST, TST, or HST and can be located in the topset, foreset, or bottomset of a clinoform (Kerans and Kempter, 2002; Catuneanu, 2006), though higher order sequences may not be recognized as distinct systems tracts (Miller et al., 2013a). I interpret three higher order sequences within the overall Kw2a sequence, which is then by definition a composite sequence (e.g. Miller et al., 2013a). Onshore composite Kw2a sequence appears to correlate with composite m5.4 sequence based on biostratigraphy and Sr-isotope age estimates. However, the onshore sequences have only provisionally been physically correlated to the offshore sequences using seismic profiles and these correlations and their age relations have not been evaluated in view of Expedition 313 drilling on the inner-middle shelf (Mountain et al., 2010), especially the integration of Sr-isotope and biostratigraphy (Browning et al., 2013).

The primary objectives of this thesis are to test the hypothesis that Kw2a is actually a composite sequence and to correlate Kw2a sequence with its proposed equivalent composite m5.4 sequence at Expedition 313 site, where the clinoform reaches its maximum thickness. To this end, I evaluated the concept of higher order sequences by analyzing the Kw2a sequence and tested a whether a physical correlation could be established between 150X and 174AX coastal plain coreholes and middle to outer shelf Expedition 313 site coreholes. To achieve the first goal, I integrated core lithology, semi-quantitative benthic foraminifera paleobathymetrical estimates, and gamma ray log data in a sequence stratigraphic framework. Integration of these three data sets enabled me to define stratal surfaces [sequence boundary (SB), transgressive surface (TS), and maximum flooding surface (MFS)] (Fig. 3), delineate stacking patterns, and infer system tracts, paleodepositional environments, and paleobathymetry in a sequence stratigraphic framework for the late early Miocene composite Kw2a sequence. To achieve the second goal, I projected the overlying and underlying sequence boundaries of composite Kw2a sequence to offshore seismic profiles (see "Seismic Interpretation and Gamma Ray Log Correlation" section) to tie the onshore log and offshore seismic data.

2 Methods

2.1 Lithology, Lithofacies, and Paleodepositional Interpretation

Core interpretation plays an important role in deciphering physical erosional surfaces (sequence boundaries, ravinement surfaces, sharp lithological contacts), gradual lithofacies changes (shifting of paleodepositional environments), and stacking patterns (fining or coarsening upward succession). The first part of physical core interpretation is to determine sequences by interpreting the underlying and overlying sequence boundaries. Therefore, I reevaluated the composite Kw2a sequence in CMZ and OV cores with respect to physical stratigraphic criteria. Miocene sequence boundaries are interpreted in cores using a variety of criteria including identification of an erosional surface. Sequence boundaries typically have rip-up clasts of the underlying material reworked into the overlying succession and may have large and long burrows filled with the overlying lithology in the underlying succession. Sequence boundaries are often associated with indurated zones that can be either above or below the surface. Other features associated with sequence boundaries onshore include: the presence of a basal shell lag and an abrupt lithofacies change indicating a change from shallower paleoenvironments below to deeper paleoenvironments above (Miller et al., 1997; Miller et al., 2001; Browning et al. 2006, Catuneanu, 2006).

In some cases, other stratal surfaces (TS, MFS) might show similar features as sequence boundaries (Browning et al., 2006). For example, the transgressive surface merges with the underlying sequence boundary where LST thins and pinches out in topset locations (Fig. 2). Shell beds, erosional contacts, and burrows might be seen at a transgressive ravinement surface as well (Miller et al., 1998; Catuneanu, 2006; Browning et al., 2006). Therefore, more than physical evidence is needed in order to confirm that an erosional surface is in fact a sequence boundary. Identification of a hiatus across a surface provides a means of confirming a sequence boundary. Therefore, I used previously published Miller et al. (2001 and 2005) Sr-isotope age estimates to evaluate hiatuses.

I collected data on the relative abundance of minerals in samples to interpret paleodepositional environment and its proximity to the shoreline. The abundance of quartz, carbonate (mostly shells and shell fragments), and glauconite fractions were visually estimated using a binocular microscope. In addition, the abundance of mica and lignite provide evidence about the proximity of a deltaic source. On the other hand, abundant carbonate shows marine influence rather than deltaic dominance in shelly and glauconitic facies (Bhattacharya, 2006). Delta front and prodelta environments contain greater amounts of lignite and mica than marine shelf environments. It is often thought that deltaic depositional environments and shelf successions are mutually exclusive, but recent developments in clastic shelf studies, for instance, show that prodelta/offshore, and delta front/shoreface facies are in connection and might switch from one to another according to interplay between sediment input, base-level changes, and marine productivity (Van Wagoner et al., 1990; Miall, 1991; Bhattacharya, 2006).

Quantitative grain-size study is applied on samples in order to calculate clay and silt (mud) versus very fine, fine, medium, coarse sand, and granule fractions. I used grain size data from Miller et al. (2001, 2005) that were collected every 5 feet. In addition to these samples, I collected 39 new samples (32 from CMZ, 7 from OV coreholes). The new samples were left in the oven for ~24 hours to dry. The samples were weighed, soaked in sodium metaphosphate (5.5 g/l) for ~30 minutes then washed through a 63 µm sieve and the mud fraction discarded. After washing, the samples were dried for ~24 hours in an oven. The samples were then sieved through 125 µm, 250 µm, 500 µm, 1 mm, and 2 mm size fractions and the sediments in each fraction were weighed.

2.2 Gamma Ray Log Interpretation

Gamma ray log data are collected by wireline logging into drill holes. The aim of this type of logging is to measure gamma radiation caused by the occurrence of naturally radioactive elements including uranium, thorium, and potassium (found especially in glauconite). Downhole gamma ray logs potentially provide a mean to identify sequence boundaries. Gamma ray peaks are associated with sequence boundaries and maximum flooding surfaces because radioactive elements found in mud and glauconite are associated with these stratal boundaries (Vail and Wornardt, 1990; Miller et al., 2001; 2005). Therefore, I correlated sharp gamma ray log peaks with the sequence stratigraphic boundaries.

In intervals with low core recovery, gamma ray log data provides better resolution and accuracy on determining not only general coarsening/fining lithological trends, but also sharp lithofacies boundaries. Within these sections gamma ray log data provides general coarsening (sand dominated), and fining (clay-silt dominated) upward patterns.

2.3 Benthic Foraminiferal Biofacies Paleodepth Distribution

Miller et al. (1997) assigned paleodepths for benthic foraminifera biofacies found on the Miocene New Jersey shallow paleoshelf. In this study, a semi-quantitative analysis was used to recognize these benthic foraminifera biofacies so that I could estimate the paleobathymetry of the paleoshelf. The distribution of benthic foraminifera changes as a function of depth on the shelf. Paleoenvironmental conditions, such as organic carbon flux, dissolved oxygen content, temperature, salinity, and turbulence (Van der Zwaan et al., 1999; Leckie and Olson, 2003) all change regularly as a function of the water depth. Thus, benthic foraminifera follow these ecologic parameters and can thus be related to paleodepth.

Paleowater depths were interpreted using two methods. A wave dominated shoreline model was adapted from Miller et al. (1997), Browning et al. (2006), Mountain et al. (2010), and Katz et al. (2013) to interpret paleowater depths. After interpreting paleoenvironments from core lithologies paleowater depths are assigned as follows: foreshore: ~0 m; upper shoreface: 0-5 m; lower shoreface: 5-10 m; shoreface-offshore transition: 10-20 m; and offshore environments: greater than 30 m.

Miller et al. (1997) developed a shallow shelf bathymetric zonation for New Jersey Miocene paleoshelf using benthic foraminiferal biofacies assuming 1:1000 shelf gradient. Predominant biofacies are assigned to certain paleodepths: *Elphidium sp.* for 0-10 m (innermost neritic), *Hanzawaia hughesi* for 10-25 m (inner neritic), *Nonionella pizarrensis* 25-40 m, *Nonionella grateloupi* 35-50 m (inner to middle neritic), *Bulimina gracilis* 50-80 m (middle neritic), and *Uvigerina sp.* 75-100 m (middle neritic) (Miller et al., 1997b and Katz et al., 2013).

I interpreted benthic foraminiferal biofacies using relative abundance data and total number of specimens per sample versus sample weight (#/g). I used the Miller et al. (1997b) benthic biofacies versus paleodepth distribution model (as modified by Katz et al., 2013) to construct paleobathymetric curves for the composite Kw2a sequence in

CMZ and OV coreholes. Furthermore, I used percent planktonic foraminiferal abundance as a supplementary paleowater depth proxy to benthic biofacies paleodepth distribution. The greater than 150 μm sediment fractions were analyzed thoroughly under binocular microscope targeting at least 300 specimen/sample (Browning, et al., 2006; Miller et al., 1997b). Samples rich in benthic foraminifera were split into fractions with a splitter until at least 300 specimens were reached. In poorly fossiliferous samples, all benthic and planktonic foraminifera specimens greater than 150 μm were picked. I utilized a semi-quantitative analysis on relative abundance of species to interpret biofacies because out of 91 samples, only 7 of them contained the target of 300 specimens. Samples containing more than 20 benthic foraminifera specimens were included in the semi-quantitative analysis for construction of a paleobathymetric curve (Katz et al., 2003; Katz et al. 2013).

I assigned particular paleodepths for predominant biofacies by following Miller et al. (1997), Katz et al. (2003), and Katz et al. (2013). Miller et al. (1997) inferred that *P. grateloupi* biofacies representative of 35-50 m, whereas *P. pizarrensis* biofacies dominates 25-40 m paleodepth for two the most common species of New Jersey shallow shelf. In this study, I chose to lump them under *Pseudononion* spp. (Miller et al., 1997) and assigned a paleodepth range of 25-50 m. *Bolivina* spp. are also another key taxa on the Miocene New Jersey shallow shelf (Miller et al., 1997; Katz et al., 2013). However, none of the samples in composite Kw2a sequence contain *Bolivina* spp. as a dominant taxon. Furthermore, I found out that the abundance of *Bolivina* spp. covaries with the number of *Bulimina* spp. Therefore, I interpreted that *Bolivina* spp. also represent similar a middle neritic paleobathymetry (50-80 m) as *Bulimina* spp. (Miller et al., 1997).

Elphidium spp. is an important benthic foraminiferal biofacies not only because they represent shallow, marginal marine environments, but also the dominance of *Elphidium* spp. is restricted to bays, lagoons, and the shallow shelf (0-10 m) (Miller et al., 1997; Katz et al., 2013). *Lenticulina* spp. were treated as indication of marine environment, but their wide depth range makes these taxa not useful for paleobathymetric analyses (Katz et al., 2013). I differentiated *B. elegantissima* from *Bulimina* spp. because Pekar and Kominz (2001) reported that *B. elegantissima* represents inner neritic paleodepths (10-25 m) in New Jersey Oligocene successions. Moreover, I observed that the abundance of *B. elegantissima* coincides with the dominance of the *Hanzawaia* spp. biofacies. Leckie and Olson (2003) found an association of *Buliminella* spp. and *Hanzawaia* spp. Therefore, *B. elegantissima* is considered to represent inner neritic (10-25 m) paleodepths in this study. *Uvigerina* spp. was assigned to the deepest paleodepth range (75-100 m) of among all benthic foraminifera biofacies. They typically are associated with MFS and mud peaks (Loutit et al., 1988; Miller et al. 1997; Katz et al., 2013). Other deeper (100-200 m) New Jersey shelf Miocene paleodepth representatives (*Cibicides pachyderma, Cibicides primulus, Oridorsalis umbonatus)* are sparse in the composite Kw2a sequence of CMZ and OV coreholes.

Benthic foraminiferal species were identified using the taxonomies of Baker (1960), Cushman and Cahill (1933), and Snyder et al. (1988). I generally identified and counted benthic foraminifera to the genus level because lumping appears appropriate in cases where more than one species resemble each other in a generic biofacies. For instance, *B. gracilis* and *B. elongata* share similar morphologies with respect to chamber length-to-width ratio, and having depressed sutures. On the other hand, *B. curta* has vertically elongated chambers that are puffier (Katz et al., 2013), but abundance of too many intermediate forms convinced me to lump them together under genus level. Furthermore, many samples have high dominance of particular genus; for example: *Elphidium poeyanum* is abundant for *Elphidium* spp., *Hanzawaia concentrica* for *Hanzawaia* spp., *Bulimina gracilis* for *Bulimina* spp., *Pseudononion pizarrensis* for *Pseudononion* spp., and *Uvigerina peregrina-Uvigerina modeloensis* for *Uvigerina* spp. In addition, Leckie and Olson (2003) suggested that determining the predominant genus is more effective and useful for neritic biofacies than using species data. As a consequence of this approach, I was able to include more species for total number of species versus sample weight (#/g) paleodistribution model.

2.4 Onshore-Offshore Well Log Projections and Seismic Correlation

In this study, the composite m5.4 sequence was physically traced on seismic profiles that were collected by three different cruises (Fig. 1): R/V *Maurice Ewing* 9009 (Ew9009), R/V *Oceanus* 270 (Oc270), and R/V *Cape Hatteras 0698* (CH0698). Ew9009 data were collected using a six-airgun source that provided deep penetration and low frequency (20-80 Hz) and generated multichannel channeled seismic (MCS) data with moderate (15 m) vertical resolution (Mountain and Miller, 1994). Oc270 data and CH0698 were collected with a higher resolution system, yielding about ~ 5 m vertical resolution. The CH0698 survey was focused on the inner to middle shelf (Fig. 1), providing a physical connection between middle to outer shelf profiles (Ew9009, Oc270) and the onshore coastal plain and innermost shelf coreholes and well logs. Expedition 313 core data provided lithological data and age estimates tied to all three MCS grids, (Mountain et al., 2010; Browning et al., 2013; Miller et al., 2013a).

Correlation of onshore well log data to offshore seismic profiles depends on assumptions and approximations. I imported the log data by using a time-depth (T-D) chart created from middle to outer shelf seismic data to correlate the seismic profiles with well crossed by the grids (e.g., ACOW1, ACOW2, and AMCOR 6011). For onshore sites [Cape May (CM), Cape May Zoo (CMZ], Sea Isle City [SIC], OV, Strathmere, and AC], I projected the coreholes and well logs using an estimated a uniform dip gradient and the T-D function. The T-D function (Mountain et al, 2010) was generated from the Expedition 313 area and adapted to inner shelf seismic profiles to import well log data onto the nearest seismic profiles on Seismic Micro Technology (SMT) software. Even though the T-D chart was generated from the inner to middle shelf seismic data (Fig. 1), it appears applicable to the inner-innermost shelf seismic profiles (see "Seismic interpretation and Gamma Ray Log Correlation" section).

Projection of onshore wells and coreholes was done using Minimum Distance Method. The method basically assumes no vertical change in thickness from the well to the seismic profiles (ranging from 0.7 km at AC to 10.1 km at CMZ) and displays the log on the nearest seismic line. In this method, the nearest seismic line is automatically determined by projection of an imaginary perpendicular line from corehole to the seismic line. Projection from the wells and coreholes to the seismic profiles required an estimate of the general dip gradient.

I chose CH0698 lines 5 and 9 to estimate the general gradient for Kw2a sequence because they both occur parallel to the lower Miocene strata dip direction (NW-SE) and link locations to be projected (Fig. 4). Tracing of sequence boundaries bracketing the m5.4 sequence from the Expedition 313 area shows two uniform reflections with high impedance contrasts (Fig. 5). The reflections were traced 5.9 and 10.8 km on CH0698 profiles 5 and 9 respectively. I assumed 1775 m/s average velocity for unconsolidated sediments around 0.2-0.3 s two way travel time (G.S. Mountain, personal communication, 2013) and I estimated ~62.3 m vertical downdip gradient for the Kw2a sequence in 10 km lateral distance (Table 2). Moreover, I also estimated ~ 2.5 m thickening for the Kw2a sequence, which is below vertical resolution of CH0698 seismic data; therefore, thickening wasn't included in the well log projections and strata are assumed to have uniform thickness along dip direction (SE).

3 Results

3.1 Cape May Zoo Corehole Interpretation

I placed the basal composite Kw2a sequence boundary, the boundary between Kw1c and Kw2a1, at the base of an indurated, burrowed, shelly sandstone at 630.7 ft (192.2 m) at Cape May Zoo. The indurated sandstone lithology continues from the sequence boundary up to 628.0 ft (191.4 m). Above this zone, I observed quartz granules and pebbles interpreted as fragments from the indurated bed (Fig. 7). In fact, the whole indurated zone (630.7-628 ft) (192.2-191.4 m) is interpreted to represent a sequence boundary.

I sampled the indurated zone to analyze benthic foraminiferal abundances and define the stacking pattern, but the indurated rock would not fully disaggregate. I was able to recover ~2 grams of sediment, which did not contain foraminifera. The absence of benthic foraminifera may be evidence of subaerial exposure and a non-marine environment of deposition or dissolution during diagenesis (see “Discussion” section). The sample from 627.6 ft (191.3 m) contains only five *Hanzawaia* spp. and one *Textularia* spp. with low foraminiferal abundance (0.5 #/g), which is not enough to include in the semi-quantitative analysis. The sample from 626.9 ft (191.1 m) is interpreted as a FS based on a minor gamma ray peak and abundant benthic foraminifera (245 specimens), an order of magnitude increase in benthic foraminiferal abundance; 5.4 (#/g), and six planktonic foraminifera (2.4%), that suggest a shift to deeper water. The dominance of *Hanzawaia* spp. (87.4%) indicates deposition in inner neritic paleodepths (10-25 m; *Hanzawaia* biofacies). The sample at 626.0 ft (190.8 m) contains 348 benthic and 15 planktonic foraminiferal specimens (4.1% of the total abundance). Benthic foraminifers are dominated by *Hanzawaia* spp. (73.9%), *Spiroplectammina carinata* (10.9%), and *Uvigerina* spp. (4.9%). The occurrence of *Uvigerina* spp. is taken to indicate a possible deepening within the *Hanzawaia* (10-25 m) biofacies. Even though the indurated zone restricts grain size analysis, examination of the cores shows a coarsening upwards succession (Fig. 7). From a sequence stratigraphic point of view, coarsening upwards can be correlated with late stage of LST (see "Discussion" section). This inferred LST includes a FS and is underlain by a SB and overlain by a TS at 625.0 ft (190.5 m). At 621.0 ft (189.3 m) the predominant benthic foraminiferal biofacies changes from the shallower inner neritic (10-25 m) to the relatively deeper (25-50 m) inner to middle neritic environment, which supports deepening from 626.9 to 621 ft (191.1-189.3 m). The grain size fines upsection in this interval, consistent with the deepening upward interpretation based on benthic foraminifers. I identified a TS at 625.0 ft (190.5 m; Fig. 7) at a positive gamma ray log peak at about the level that abrupt deepening and fining upsection begins (Fig. 6). Thus, the ~5.3 feet interval between 630.7 ft (192.2 m) to 625.0 ft (190.5 m) represents a coarsening upwards LST succession with a basal indurated sandstone and overlying non-lithified coarser sediments. The indurated sandstone might represent a backshore-foreshore depositional environment because no foraminifers are present and the coarse sediments above erosional surface are correlateable with the intertidal zone. Conversely, the non-lithified, upper portion of the LST represents shoreface-offshore transitional environment with medium to coarse quartz sand and inner neritic, 10-25 m paleodepth.

The sample at 621.0 ft (189.3 m) has 29.8 #/g of foraminifera and the benthic assemblage is dominated by *Pseudononion* spp. (44.4%), *Hanzawaia* spp. (30.6%), *Bulimina* spp. (11.1%), and *Uvigerina* spp. (6.9%). The sample at 620.3 ft (189.1 m) is devoid of foraminifera. I observed secondary gypsum crystals in those samples that might indicate dissolution of carbonate shells. In addition, I noted that organic matter was abundant below this and decreases between 621.0 ft (189.3 m) and 620.3 ft (189.1 m), suggesting a change from laminated prodelta clay below to mud dominated offshore facies above.

Two flooding surfaces occur at 618.0 ft (188.4 m) and 610.0 ft (185.9 m) in the middle part of the TST. The lower flooding surface in inferred from a gamma ray log peak and finer grained facies. At the upper flooding surface, there is a gamma ray log peak and abrupt shift to finer grain sized facies going up section. The sample from 611.0 ft (186.2 m) has 11.0 #/g benthic foraminifera with *Pseudononion* spp. (73.3%) dominating. The upsection increase in percent *Pseudononion* spp. within the *Pseudononion* biofacies supports deepening upward in the TST, even though, it occurs within a general inner to middle neritic paleobathymetric zonation. Above 611.0 ft (186.2 m), the TST mainly consists of massive muddy sediments without any observable benthic foraminifera up to 581.0 ft (177.1 m) where the fining upwards trend stops. At 606.0 ft (184.7 m), 591.0 ft (180.1 m), and 586.0 ft (178.6 m) the samples were barren with respect to benthic or planktonic foraminifera due to mud-predominant lithofacies. Only the sample at 601.0 ft (183.2 m) contains 11 specimens with 1.9 #/g abundance, which wasn't enough to include semi-quantitative benthic foraminifera analysis (Table 3).

The MFS is placed at 581.0 ft (177.1 m) where a general coarsening upwards trend begins and there is a shift from offshore to prodelta muds above. The MFS coincides with the highest benthic foraminifera abundance (70.0 #/g) and a benthic foraminiferal assemblage dominated by *Uvigerina* spp. (52.3%) and *Pseudononion* spp. (47.6%), and 4.6% planktonic foraminifera. Both benthic and planktonic foraminiferal abundances support that the deepest (75-100 m) paleodepths for composite Kw2a sequence are reached at 581.0 ft (177.1 m). Unfortunately, the gamma ray log does not provide a distinct peak at the MFS because mud facies dominate ~90% of the section starting at 590.0 ft (179.8 m) up to 563.5 ft (171.8 m). However, it is possible to detect the onset of a general coarsening upward trend above the MFS in cumulative grain size chart. Even though MFS at is associated with a mud peak and onset of a coarsening upward succession, the boundary differs from any SB because it is also associated with deepest *Uvigerina* spp. biofacies and relatively conformable succession through TST to HST. Benthic foraminiferal biofacies show a clear shallowing up section pattern above the MFS. *Uvigerina* spp. percent peaks at the MFS. Above this, at 576.0 ft (175.6 m) benthic foraminifera are 43.6 and #/g and are dominated by *Pseudononion* spp. (57.5%), *B. elegantissima* (19.2%), *Bulimina* spp. (5.5%), *Bolivina* spp. (4.6%), with 5.9% planktonic foraminifera abundance. The foraminiferal data indicate shallowing upsection to inner to middle neritic paleodepths (25-50 m) above the MFS. The shift is abrupt because the expected *Bulimina* spp.-*Bolivina* spp. biofacies zone (50-80 m) is overstepped between the *Uvigerina* spp. and *Pseudononion* spp. biofacies. Other samples from, 571.0 ft (174.0 m) and 566.0 ft (172.5 m) contain only 13 and 9 specimens, respectively. Both samples suggest a continuation of the *Pseudononion* spp. biofacies in mud dominated prodelta facies.

Abundant bivalve and gastropod shell fragments and coarser-grained lithofacies occur between 563.5 ft (171.8 m) and 561.0 ft (171.0 m), in contrast to the underlying and overlying mud dominated prodelta facies. I propose three possible scenarios for deposition of this interval: a delta lobe switch, channel fill deposition, or redistribution of sediments. The ~2.5 ft (0.8 m) interval correlates with expected thin channel fill deposits, but channel fill deposit should display physical evidence for erosion, including an uneven basal surface. However, there is no distinct surface at either the lower or the upper boundary of the coarser-grained interval. Moreover, channel deposits fine upwards, yet the reverse is observed in this interval. Thus, a channel interpretation is not preferred. Conversely, the former proposed scenario (delta lobe switch) seems to fit the data because this coarser interval overlies and underlies prodelta facies within *Hanzawaia* spp. predominance. But, the ~2.5 ft (0.8 m) interval is a product of small-scale process compared to delta lobe switch and this interval represents a discrete sedimentary record between two finer grained depositional settings. An abrupt lithologic change without any discernable uneven surface, and not having transported benthic foraminifera strengthen and favor redistribution of sediments with wave activity, but in a very limited small scale. This zone also marks a boundary between mud-dominated lower and slightly coarser grained upper HST of Sugarman and Miller (1993). The overlying upper HST shows a fining upwards trend between 561.0 ft (171.0 m) and 549.8 ft (167.6 m) and comprises dark brownish, more fine sand bearing prodelta to finer (cm scale) laminated, greenish color facies. *B. elegantissima* (42.5%), *Bolivina* spp. (26.0%), and *Hanzawaia* spp.

(23.3%) dominate the biofacies at 561.0 ft (171.0 m). The other two samples from the upper HST are dominated by *Hanzawaia* spp. (64.6%), *Pseudononion* spp. (7.8%), and *Bulimina* spp. (5.8%) at 556.0 ft (169.5 m), and *Hanzawaia* spp. (37.4%), *Bulimina* spp. (25.3%), *Pseudononion* spp. (8.8%) at 551.0 ft (168.0 m). Therefore, a general shallowing upward trend from *Uvigerina* spp. to *Hanzawaia* spp. biofacies occurs in the HST of the Kw2a1 sequence (Fig. 6).

I interpreted a second sequence boundary at 549.8 ft (167.6 m) that separates Kw2a1 and Kw2a2 higher order sequences. This boundary marks an abrupt contact between fossiliferous, finely laminated mud-dominated prodelta facies below and barren, very fine, fine sand dominated shoreface offshore transitional facies above. The sequence boundary is associated with a 0.5 ft burrowed zone containing rip up clasts. Moreover, a shelly layer marks the uppermost level of the burrowed zone associated with the sequence boundary. No LST is identified for the Kw2a2 sequence because the succession starts with a fining upward trend above the Kw2a2 sequence boundary. In other words, the TS immediately overlies and merges with the sequence boundary. Absence of a LST might be a result of landward side (topset) placement of the core with respect to the basin (see “Discussion” section). Unfortunately, neither benthic nor planktonic foraminifera were recovered from higher-order Kw2a2 sequence for semi-quantitative analysis. Thus, I used the gamma ray log data and cumulative grain size data to interpret the sequence. In order to subdivide the TST from the HST, 32 additional samples were collected between 549.0 ft (167.3 m) and 533.5 ft (162.6 m) with a 0.5 ft sampling interval (Fig. 8). These samples were analyzed with respect to their grain size to construct a more precise cumulative grain size curve for the Kw2a2 sequence (Fig. 8). The TST is mainly comprised of mud, very fine, and fine sand with some medium, and coarse sand fraction decreasing up to 543.5 ft (165.5 m) (Fig. 8). Therefore, I placed the MFS at 543.5 ft (165.5 m) where the percentage of mud in the sample reaches its maximum peak (31.30%) and above which there is a general coarsening upward trend. Moreover, the very fine sand fraction increase upsection and reaches its maximum point at 543.5-543.0 ft (165.7-165.5 m) and then starts a drastically decreasing trend upsection (Fig. 8). Above the MFS, the HST coarsening upwards to the upper sequence boundary at 531.2 ft (161.9 m) that divides Kw2a2 and Kw2a3 sequences.

Miller et al. (2005) placed a third higher order sequence boundary between Kw2a2 and Kw2a3 at 529.5 ft. based on a gamma ray peak at that level, but the proposed sequence boundary lies within a 2 foot coring gap that prevented lithofacies and biofacies analyses. I propose placing the sequence boundary at 531.2 ft (161.9 m) because a shell bed marks this level as the sequence boundary (Fig. 9). In addition, gamma ray log values generally increase upsection, which points to the onset of a general fining upward trend at that level, interpreted as a TST. In spite of an absence of foraminifera in the TST, the log character suggests merging of the transgressive surface with the higher order sequence boundary. In the TST, both gamma ray log values and cumulative grain size fraction data show a solid fining upward trend up to 520.0 ft (158.5 m). Above that level, gamma ray log data and cumulative grain size data show coarsening upward trends (Fig. 6) that indicate the HST. The sample at 515.9 ft (157.3 m) contains 222 benthic foraminifera specimens dominated by *Hanzawaia* spp. (48.2%) suggesting inner neritic (10-25 m) paleodepths. In addition, *Pseudononion* spp. (43.7%) and 3.2% planktonic foraminifera suggests deposition in the deeper parts of the inner neritic zone. It is not possible to prove a shallowing upwards succession using foraminfiera through the higher order Kw2a3 sequence because the sample at 515.9 ft (157.3 m) is the only one that contains enough foraminifera to conduct semi quantitative analysis.

The uppermost sequence boundary that separates Kw2a3 and Kw2b is interpreted at 515.7 ft (157.2 m). The sequence boundary is marked by a sharp lithologic contact that is an erosional surface containing coarse grains of the underlying material into the overlying Kw2b sequence. An abrupt gamma ray log peak marks the sequence boundary. Kominz et al. (unpublish) suggested Sr-isotope age estimates of 16.4 Ma for 524.8 ft (160.0 m) and 15.9 Ma for 512.0 ft (156.1 m) giving a hiatus of 0.5 m.y. across the boundary.

3.2 Ocean View Corehole Interpretation

The lowermost sequence boundary of Kw2a at the Ocean View corehole is placed at 640.4 ft (195.2 m) as in Miller et al. (2001) because Kominz et al. (unpublished) Sr-isotope age estimates show a time gap of 1.7 m.y. across the sequence boundary. The underlying Kw1b sequence has an age estimate of 19.2 Ma at 641.0 ft (195.4 m) and higher order Kw2a1 sequence has a Sr-isotope age estimate of 17.5 Ma at the SB. There is no major lithofacies change and only a small gamma ray log peak at this level. The placement of the sequence boundary is supported by the presence of a one-inch (2.5 cm) thick shell bed at 640.4 ft (195.2 m).

No foraminifers were recovered from finely laminated, mud dominated, lignite rich facies at the base of the sequence (640.4 ft to 631.0 ft; (195.2 m-192.3 m), which might suggest deposition in non-marine to marginal marine environment. The organic-rich sediments may indicate marsh paleoenvironments (Fig 10; Miller et al., 2001). A sample from 636.4 ft (194.0 m) indicates a flooding surface at 636.4 ft (194.0 m) with bivalve shells and lighter gray color (inferred lower organic matter) than was found in the underlying mud-dominated organic-rich facies. Moreover, this flooding surface marks the boundary between barren possible marsh sediments below and shell rich innermost neritic lithofacies above. Neither planktonic nor benthic foraminifera were recovered from the neritic sediments. Upsection, the sediments become increasingly marine influenced with more carbonate and glauconite and less organic matter. Another flooding surface at 631.0 ft (192.3 m) shows abrupt deepening to inner to middle neritic paleodepths (25-50 m), dominated by *Pseudononion* spp. (38.5%), *Hanzawaia* spp. (29.5%), and *Uvigerina* spp. (11.1%) and 56.5 #/g total benthic foraminifera abundance. In spite of evidence for abrupt deepening, the gamma ray log character and lithological pattern do not show a clear fining upward trend as expected in a TST. The sample from 628.0 ft (191.4 m) shows shallowing upward with 9.4 #/g total benthic foraminifera abundance and a biofacies dominated by *Hanzawaia* spp. (37.8%), *Pseudononion* spp. (28.6%), and *Uvigerina* spp. (19.4%). No distinct coarsening upward occurs from 640.4 ft (195.2 m) to 628.0 ft (191.4 m), but fining upward begins at the latter level. Therefore, the succession is considered to be LST from the sequence boundary at 640.4 ft (194.0 m) to 627.0 ft (191.1 m) with high organic content of dark colored, finely laminated clay interpreted as marsh facies at the bottom and innermost to inner neritic lithofacies at the top. From sequence stratigraphic point of view, deepening upsection can be explained by slowly rising sea-level and moderate to high rate of sedimentation, which exceeds increasing rate of accommodation space by base-level rise (Neal and Abreau, 2009).

I interpret the section from 627-601 ft (191.1-183.2 m) as the TST. Deepening is indicated by the sample at 626.0 ft (190.8 m) assigned to inner to middle neritic (25-50 m) paleodepths based on abundant benthic foraminifera (39.4 #/g) dominated by *Pseudononion* spp. (70.6%), *Hanzawaia* spp. (18.7%), and *Bulimina* spp. (5.0%). Moreover, the second highest planktonic foraminifera peak (3.8%) within the entire higher order Kw2a1 sequence occurs in this sample. Cumulative grain size data and gamma ray log values show fining upsection between 628.0 ft (191.4 m) and 626.0 ft (190.8 m), indicating the base of the TST. Therefore, I propose that a pale light gray indurated calcareous claystone (Fig. 11) marks the boundary between LST and TST as TS at 627.0 ft (191.1 m). Above the TS, it is also possible to observe rip up clasts between 627.0 (191.1 m) and 626.7 ft (191.0 m). The facies above the TS represent a finely laminated micaceous clay dominated facies, which suggests inner to middle neritic paleoenvironments with deltaic influence.

The sample from 621.0 ft (189.3 m) indicates a shallowing within the overall transgressive TST. This is based on reduced abundances of total benthic foraminifera (26.8 #/g) and dominance of *Hanzawaia* spp. (47.6%), *Lenticulina* spp. (18.5%), *Uvigerina* spp. (12.9%) that suggest shallowing to inner neritic (10-25 m) paleoenvironments. In the overlying TST foraminifera are rare in the mud-dominated lithofacies. Some samples are barren of foraminifera; for example, the sample from 616.0 ft (187.8 m) includes only two benthic specimens in the greater than 150 µm size fraction. On the other hand, in spite of high clay content, foraminifera become abundant at what are interpreted as flooding surfaces. For instance, at 611.0 ft (186.2 m) I found the highest benthic foraminifera peak with, 4750.0 #/g comprising *Hanzawaia* spp. (68.2%), *Pseudononion* spp. (10.7%), and *Lenticulina* spp. (7.8%) indicating inner neritic (10-25 m) paleodepths. Therefore, I assume that paleodepths do not change in this barren zone. At 606.0 ft (184.7 m) in spite of two orders of magnitude lower (96.7 #/g) foraminiferal abundance, I observe deepening-upward succession because this sample contains *Pseudononion* spp. (60.7%), *Hanzawaia* spp. (17.9%), and *Uvigerina* spp. (14.3%).

The second highest numerical peak for benthic foraminifera is reached at 601.0 ft (183.2 m) with 1564.8 #/g. The sample is dominated by the deepest benthic foraminifera biofacies assemblage including *Uvigerina* spp. (46.8%), *Pseudononion* spp. (26.5%), and *Hanzawaia* spp. (21.0%) suggesting middle to outer neritic (75-100 m) paleodepths. Moreover, the second deepest (50-80 m) benthic biofacies representative, *Bolivina* spp. is qualitatively abundant in the 63-150 μm size fraction. Even though gamma ray log data does not provide a major peak, benthic foraminifera biofacies does show the beginning of a shallowing upwards trend above this level. I place the MFS at 601.0 ft (183.2 m), representing the boundary between the fining upward TST and coarsening upward HST.

The HST occurs from the MFS at 601.0 ft (183.2 m) to the upper sequence boundary at 531.2 ft (161.9 m). Above the MFS, total benthic foraminiferal abundance dramatically drops to 100.8 #/g dominated by *Pseudononion* spp. (38.9%), *Uvigerina* spp. (35.9%), and *Hanzawaia* spp. (20.6%). The biofacies distribution supports a shallowing upward to inner to middle neritic paleodepths (25-50 m) at 596.0 ft (181.7 m). Above this first regression, the HST aggrades and offshore clays dominate the section from 595.0 ft (181.4 m) to 560.0 ft (170.7 m). The sample from 586.0 ft (178.6 m) contains 22.1 #/g benthic foraminifera abundance dominated by *Pseudononion* spp. (85.7%), *Hanzawaia* spp. (7.1%), and *Uvigerina* spp. (2.4%) interpreted as a continuation of inner to middle neritic (25-50 m) paleodepths. Above this, the HST is almost barren of foraminfera in the >150 μm size fraction up to 546.1 ft (166.5 m). Qualitative analysis of the 63-150 μm fractions between 586-546 ft (178.6-166.5 m) shows that *Pseudononion* spp.*, Uvigerina* spp.*,* and *Hanzawaia* spp., dominate the assemblage between 581.0-566.0 ft (177.1-172.5 m). Above 566.0 ft (172.5 m) the 63-150 μm size fraction only contains rare specimens of *B. elegantissima* (inner neritic paleodepth (10-25 m) indicator). Thus, I assume that this barren interval represents a gradual shallowing upward zone from inner to middle neritic (25-50 m) *Pseudononion* spp.*,* dominant environment to *Hanzawaia* spp. and *B. elegantissima* dominant inner neritic (10-25 m) zonation.

From a lithologic point of view, mud dominates the lower part of the HST and fine sand percentages slowly increase upsection. At 551.0 ft (167.9 m) there is a change from a mud dominated aggradational to sand dominated progradational stacking pattern. I suggest this change from barren, inner to middle neritic facies, below, to fossiliferous inner neritic facies, above, is the boundary separating the lower and upper HST. At 546.1 ft (166.5 m), I interpret a shelly layer within the blocky inner neritic clay facies. This sample corresponds with an abrupt change from barren benthic foraminifera zone below to 67.8 #/g of *Hanzawaia* spp. (49.2%), *Pseudononion* spp. (39.1%), and *Uvigerina* spp. (5.2%) dominated biofacies. This sample is also important because it contains 4.4% *Elphidium* spp., which was not present lower in the Kw2a1 sequence. Above 546.1 ft (166.5 m) *Elphidium* spp. becomes more abundant upsection. For instance, at 541.0 ft (164.9 m) the sample contains 17.6 #/g benthic foraminifera of *Hanzawaia* spp. (35.3%), *Elphidium* spp. (25.8%), and *Pseudononion* spp. (22.6%). In spite of the relative percent increase in *Elphidium* spp., the dominance of *Hanzawaia* spp. suggests inner neritic (10-

25 m) paleodepths. At 536.0 ft (163.4 m) *B. elegantissima* (34.8%) is the dominant species followed by *Pseudononion* spp. (25.4%), *Hanzawaia* spp. (17.1%), and *Elphidium* spp. (11.4%). This distribution suggests stable inner neritic paleodepth (10-25 m) between 556.0 ft (169.5 m) and 536.0 ft (163.4 m).

A sharp lithologic contact at 531.2 ft (161.9 m) with heavily bioturbated, shelly fine sand below 531.7-531.1 ft (162.1-161.9 m) and mud-dominated lithology above is interpreted as the sequence boundary separating Kw2a1 and Kw2a2. A sample from 531.2 ft (161.9 m) has relatively high abundances of foraminifera (174.3 #/g) dominated by *B. elegantissima* (52.9%), *Bolivina* spp. (23.8%), and *Pseudononion* spp. (17.2%), suggesting inner neritic paleodepths (10-25 m). Even though rip-up clasts or a distinct erosional surface are not observable above 531.1 ft (161.9 m), benthic foraminifera suggest a merged sequence boundary and transgressive ravinement surface within the shelly zone. A gamma ray log minimum at the sequence boundary, increasing values upsection, a mud peak, and mud dominance up to MFS are supplementary supporting features for a merged SB-TS interpretation. Abundance of bivalve fragments and abundant carbonate also supports the merged sequence boundary/transgressive surface as well.

The TST consists of fine-grained, mud dominated facies from the sequence boundary to the MFS at 524.9 ft (161.4 m) where the boundary separates clay dominated inner neritic facies below, from inner neritic shelly, sand dominated facies above (Fig. 12). Furthermore, the blocky lithologic character above this points out an aggradational stacking pattern in the HST. Only 4 *Lenticulina* spp. and 3 *Elphidium* spp. were recovered from the sample at 515.0 ft (157.0 m). That level might mark a flooding surface in the HST because cumulative grain size data shows onset of a finer grained lithology and supports the presence of parasequence boundary. The abundance of *Elphidium* spp*., Lenticulina* spp., mud and fine sand, and abundant shell fragments suggest innermost neritic (0-10 m) paleodepths and lower to upper shoreface environments up to the overlying sequence boundary at 502.2 ft (153.1 m).

The sequence boundary that separates Kw2a2 and Kw2a3 is interpreted at an abrupt lithofacies change and gamma ray log peak at 502.2 ft (153.1 m). No foraminifers were recovered in the sample at 502.2 ft (153.1 m); however, at 500.0 ft (152.4 m), low abundances (13.6 #/g) of benthic foraminiferal dominated by *Hanzawaia* spp. (41.1%), *S. carinata* (31.7%), and *Pseudononion* spp. (19.6%), suggest inner neritic paleodepositional environment and 10-25 m paleodepth. At 496.0 ft (151.2 m), low total benthic foraminifera abundances (2.8 #/g), are dominated by a deepening upward succession with *Pseudononion* spp. (53.3%), *Hanzawaia* spp. (26.7%), and *Bulimina* spp. (16.7). Moreover, the presence of glauconite at both 500.0 ft (152.4 m) and 496.0 ft (151.2 m), suggest more marine influence supporting a deepening of the succession. Thus, I interpreted this deepening and fining upwards successions as the TST.

I identified the MFS at 495.0 ft (150.9 m) above the deepening and fining upward TST, where it is marked by a gamma ray peak and overlain by the onset of a blocky, slightly coarsening upward succession. Between 496.0-490.0 ft (151.2-149.4 m) the ratio between total sand percent suddenly shifts from 35.3% to 81.2% (Fig 10). Furthermore, a retrogradational stacking pattern in the TST changes to a generally progradational trend. The MFS separates shoreface-offshore transition facies below from prodelta facies above. The sample from 490.0 ft (150.9 m) comprises 5.1 #/g of *B. elegantissima* (35.0%), *Hanzawaia spp*. (24.5%), *Bolivina* spp. (17.48%), and *Pseudononion* spp. (16.1%). Covariance of the two most abundant biofacies, *B. elegantissima* and *Hanzawaia* spp. suggests inner neritic paleodepth (10-25 m). The section deepens from inner to middle neritic in the TST, then shallows upsection to inner neritic in the lower HST. Unfortunately, no foraminifers are present above 490.0 ft (150.9 m), but lithofacies are typical progradational (prodelta to delta front) facies up to overlying sequence boundary at 465.4 ft (141.6 m). High abundance of mica and a predominance of pure quartz sand suggest deltaic influence above the shoreface-offshore transitional facies. Mud and fine sand dominate blocky or occasionally finely laminated prodelta facies from 495.0 ft to 477.1 ft (150.9 to 145.4 m) in the lower HST. Above the lower/upper HST boundary there is an abrupt increase in the sand/mud ratio relative to the underlying mud dominated facies. A gamma ray log decrease also marks this boundary (Fig 10). Sand-dominated delta front sediments predominate up to the uppermost sequence boundary at 464.5 ft (141.6 m). The sequence boundary marks the lithofacies contact between delta front sand below and prodelta clay above. The Kw2a/Kw2b sequence boundary is a 4 ft (1.2 m) burrowed zone within finely laminated muddy prodelta facies. In addition, a gamma ray peak that is associated with abrupt fining is also observable at the sequence boundary.

3.3 Seismic Interpretation and Gamma Ray Log Correlation

This section is based on correlation of offshore seismic profiles (Fig. 1 and Fig. 4) to available onshore (ODP Legs 150X and 174AX), and offshore (ACOW-1, ACOW-2, and AMCOR 6011) coreholes and wells. I identified the Kw2a sequence on gamma ray log data and projected these wells into the nearest seismic profiles and traced basal and top Kw2a sequence boundaries through the offshore grid where the m5.4 sequence boundary was recognized (Monteverde et al., 2008; Mountain et al., 2010; Miller et al., 2013b). For this purpose, I correlated composite Kw2a sequence gamma ray log data in six onshore and three offshore well logs that was sampled the Kw2a sequence (Fig. 4) and projected the gamma ray log data onto offshore seismic profiles. In this way, a physical relationship is established between onshore upper lower Miocene composite Kw2a sequence and the offshore composite m5.4 sequence (Miller et al., 2013a). In addition higher order sequences were interpreted from gamma ray log data in CMZ, SIC, OV, AC, and ACOW-1 well logs (Fig. 13), but these cannot traced along through the offshore seismic profiles due to limits in vertical resolution.

I computed a vertical gradient needed to project the onshore wells offshore to the seismic profiles (Table 2; see “Methods” section). Moreover, the reliability of T-D function (Mountain et al., 2010) in wells crossed by the seismic profiles (see “Methods” section) (Table 1) was tested at the end of the study.

I started by constructing a gamma ray log cross section that is oblique to general strike trend (Fig. 13) based on the core control in CMZ and OV sites. I picked overlying and underlying sequence boundaries of the composite Kw2a sequence in AC, OV, CM, and CMZ well logs. Then, I correlated the gamma ray log data from these four sites with each other and other available Coastal Plain well logs such as Strathmere and SIC. These interpretations were carried into the offshore and correlated to gamma logs in wells ACOW1, ACOW2, and AMCOR-6011 (Fig. 13).

I chose AC, ACOW1, and ACOW2 well logs to project their gamma ray log data onto the seismic profiles due to three reasons: First, the well logs are located within a 10 km distance radius, which provides a more reliable correlation for similar gamma ray log data trends and peaks. Second, the spatial location of these three well logs (Fig. 4) occurs between Expedition 313 site and updip onshore coreholes (OV, Strathmere, SIC, CMZ, and CM). Last, these three coreholes are the closest to the seismic data (profiles CH0698 lines 27, 38, and 16, Fig. 4), which allows their projection without accounting for downdip gradient and/or thickening. For example, AC location is ~770 m distant from nearest CH0698 line 27, which provides a reliable projection between the log data and the seismic reflections. In addition, ACOW1 and ACOW2 were projected to CH0698 lines 38 and 16 that are 245 m and 25 m distance away, respectively. However, I adjusted the first peak of the gamma ray log data with respect to the sea floor. All these three well log projections were treated separately and traced along the CH0698 lines 27, 38, and 16 respectively. Then, the three seismic lines were loop correlated (Fig. 14) within the tight seismic grid to test if the gamma data were associated with the same level seismic reflections composite Kw2a sequence. Successful loop correlation showed that the AC, ACOW1, and ACOW2 gamma data characteristics were associated with the same seismic reflections even though, they were traced on the different seismic profiles (CH0698 lines 27, 38, and 16).

Well logs that are more than one km away from the closest seismic profile were individually projected based on the dip projection to the CH0698 lines 5 and 9 (see “Methods” section). Onshore well logs OV, Strathmere, SIC, CMZ, and CM gamma ray log data were projected onto shoreline parallel, CH0698 line 42 (Fig 4). Projection was made assuming no vertical thickness change because 2.5 m thickening in 10 km (see “Methods” section) is less than the seismic resolution of CH0968 seismic profile. After the projection, previously traced seismic reflections on CH0698 line 38 were cross-correlated with line 42. The OV, SIC, and Strathmere previously interpreted gamma ray data peaks matched with the traced seismic reflections after cross-correlation on CH0698 line 42 (Fig. 15, 16, and 17). In general, the two bounding reflectors are remarkably parallel, though I also noted where younger strata onlap to the overlying Kw2a sequence boundary in one location (Fig 18). It is also possible to observe erosional relief, a small scale eroded channel, and younger deposition that mimics the shape of eroded channel close to wells OV, Strathmere and SIC (Fig. 18).

For the onshore-offshore correlation section of my study, I traced the same seismic reflectors from ACOW1-2 and AC coreholes and correlated those to the m5.4 composite sequence using onshore and nearshore wells, and traced its bounding reflections to Expedition 313 coreholes on New Jersey mid-shelf. The upper and lower sequence boundary reflections were traced across the CH0698 seismic grids to Oc270 line 529 IODP 313 coreholes site. I traced the bounding reflections to the Oc270 line 529, looping the seismic profiles and verifying the seismic correlation of these two bounding reflections (Fig. 1). The two reflectors marking Kw2a matched with the gamma ray interpretation at the AMCOR-6011 on CH0698 line 16 (Fig. 19). I was able to physically connect the onshore Kw2a to the IODP 313 corehole where I demonstrate that Kw2a is physically equivalent to composite sequence m5.4 (Fig. 19 and 20). For correlation of the top sequence boundary of Kw2a and m5.3 seismic ambiguity occurred at landward side of M27 corehole at IODP 313 site due to approaching thicker depocenters and truncated-pinched out seismic reflections (Fig. 21) (see “Discussion” section).

To verify that the well log projections are valid, I compare the well log thicknesses of corehole and seismic profiles of the composite Kw2a sequence using the

T-D function of Mountain et al. (2010; Table 1). All well logs and seismic profile thicknesses matched within a ± 5 m vertical range, which is appropriate considering the error on ~ 5 m vertical resolution data. Compatible well log and seismic profile thicknesses showed that the T-D function developed for the middle to outer neritic data can be applied to inner shelf New Jersey seismic data. The reliability of correlation is testified by tracing the thickness of Kw2a sequence in individual well logs (Fig. 13) and then loop correlating them on seismic profiles. In this way, it is demonstrated that each of the three assumptions (see "Methods" section) not only works individually, but are also valid when integrated.

4 Discussion

A thin LST is interpreted at the bottommost part of the composite Kw2a sequence in higher order Kw2a1 sequence at both Ocean View and Cape May Zoo sites. Gamma ray logs show a serrated pattern in these LST (Fig. 6 and 10), interpreted as repetitive fining and coarsening upward successions. Neither coarsening nor shallowing upward is noted in the LST, but flooding surfaces occur. Benthic foraminifera biofacies show slightly deepening upward trends within the LST. Therefore, I suggest that the LST's might represent the late stages of LST in the composite Kw2a sequence. The two upper higher order sequences (Kw2a2 and Kw2a3) do not preserve any LST.

In both the CMZ and OV coreholes, I interpreted the lowest part of the Kw2a composite sequence as a LST because I observed physical features implying the presence of a LST. For instance, in the OV corehole, I observed organic content rich, mud-dominated, finely laminated, and barren marsh facies above the basal sequence boundary, 640.4 ft (195.2 m) to 636.4 ft (194.0 m). Above the marsh facies, I interpreted two flooding surfaces associated with inner to middle neritic benthic foraminifers *Pseudononion* spp. and *Hanzawaia* spp. Pale light gray, indurated calcareous claystone marks the TS with carbonate peak, 70.8% *Pseudononion* spp. predominance, and onset of fining upwards trend. In the CMZ corehole, the LST is a barren indurated zone overlain by coarsening upward medium and coarse sand with *Hanzawaia* spp., deposited in shoreface to offshore transition environments. A FS marks the boundary between the top of the indurated zone and inner neritic facies, a change to a fining upward trend, a positive gamma ray log peak, and deepening from the *Hanzawaia* spp. biofacies to the

Pseudonion spp. biofacies marks the TS.

Topset presence of LSTs can be explained with a late stage deposition of progradational to aggradational stacking pattern ($\delta A/\delta S < 1$ and increasing) during normal regression (Neal and Abreau, 2009). Occasional flooding surfaces might cause widespread deposition of LST's at topsets. LST recovery can also be explained by local preservation of incised channel fill deposits above sequence boundaries of CMZ and OV corehole sites (Fig. 3).

TS's overlie LST or are merged with the sequence boundaries. TST's are found in all three higher order sequences suggesting marine influence outpaced deltaic predominance and caused formation of deepening upwards and retrogradational stacking pattern.

MFS's are indicated by high benthic foraminifera abundance and dominance by *Uvigerina* spp. In zones devoid of foraminifera, I did not estimate paleodepths; however, I cannot assert that all barren zones represent non-marine depositional environments because they may be attributed to dissolution particularly in prodelta, organic-rich deposits. These zones are associated with mud facies abundance in both TST and HST. Preservation become worse in organic-rich mud facies, resulting in dissolution of calcareous tests.

I integrate the system tracts and paleodepth interpretations (Fig. 6 and 10) to suggest that spatial positions of the CMZ and OV cores were in a transitional zone between Coastal Plain (topset) and the rollover inflection point or (foreset) within the Miller et al. (2013a) clinothem model (Fig. 3). In this setting, the LST thins and the sequence boundary merges with TS. Moreover, Katz et al. (2013) mentioned that no

Elphidium spp. (<10 m) biofacies are found in lower to middle Miocene sequences in Expedition 313 sites. They reported rather deeper outer neritic depths (100-200 m) and benthic foraminifera biofacies: *Cibicidoides pachyderma, C. primulus, Hanzawaia mantaensis, Oridorsalis umbonatus.* In this study *Elphidium* spp. is recovered from upper HST's and no benthic foraminifera were observed that were deeper than *Uvigerina* spp. (75-100 m). Onshore-offshore seismic connection of the Kw2a and m5.4 sequence boundaries show that even though the depositional regimes were different, the late early Miocene sequences are physically connected. Therefore, I suggest that late early Miocene composite Kw2a onshore sequence is the shallower equivalent of deeper m5.4 sequence of Miller et al. (2013a) and Katz et al. (2013).

Miller et al. (2001, 2005) introduced Sr-isotope age estimates from below and above the higher order sequence boundaries, for example, for OV site 17.6 Ma, 17.2 Ma, and 17.0 Ma were estimated from 563.8 ft (171.9 m), 531.6 ft (162.0 m), and 502.9 ft (153.3 m), respectively. For CMZ site, 17.5 Ma, 17.0 Ma, and 17.3 Ma were estimated from 561.0 ft (171.0 m), 546.8 ft (166.7 m), and 524.8 ft (160.0 m) respectively.

It is possible to estimate the magnitude of relative base level fall for composite Kw2a sequence by integrating paleodepths and system tracts. Only four biofacies (*Hanzawaia* spp., *Pseudononion* spp., *B. elegantissima, Uvigerina* spp.) dominate. This moderate abundance and low diversity suggests that paleodepths range between subaerial exposure (<0 m) to middle neritic (75-100 m) in composite Kw2a sequence at OV and CMZ.

Different sedimentary regimes (onshore-offshore) might cause inaccuracy in application of the T-D function (Mountain et al., 2010) to coastal plain wells. But, the T-

D chart provided surprisingly favorable results in display of onshore well logs onto inner shelf seismic profiles because the true well logs thicknesses of gamma ray log and the thickness on seismic profiles (Table 1) were matched in 5 m error range.

Browning et al. (2013) provided detailed Sr-isotope ages for each sequence recovered at Expedition 313 Site M27, M28, and M29. In addition, updated Sr-isotope age estimates (Kominz et al., unpublished) for composite Kw2a sequence in OV and CMZ coreholes provides better age versus depth relationship (J. V. Browning, personal communication, 2013). Comparison of updated Sr-isotope age estimates and seismic data provides new insights for late early Miocene sedimentation history for onshore and offshore sequences because high-resolution age data provides differentiation between depositional versus non-depositional or erosional periods. According to the new Sr-isotope age estimates, higher order Kw2a1 Kw2a2, and Kw2a3 onshore sequences seem to be equivalents of m5.4, m5.34, and m5.33 higher order offshore sequences (Fig. 22). However, offshore higher order sequence m5.3 doesn’t appear to correlate with any onshore sequences above Kw2a due to a probable non-depositional or erosional period at the landward side. Sr-isotope age estimates imply that landward side was subjected to a longer non-depositional period than the basinward side. Above m5.3 sequence, the m5.2 sequence is correlateable with Kw1c and Kw1b higher order sequences at OV and CMZ sites (Fig. 22). A possible explanation is that relatively continuous basinward side deposition produces additional depositional-non-depositional periods than landward side equivalents. It causes deposition of an extra higher order sequence m5.3, offshore.

Physically it is shown that the onshore-determined basal sequence boundary of composite Kw2a sequence definitely correlates with basal sequence m5.4 seismic reflection Miller et al. (2013a). It appears that the upper sequence boundary of Kw2a correlates with sequence boundary with either m5.3 or m5.2 at Expedition 313 sites. My seismic tracings are a half cycle offset from Mountain et al. (2010) and Miller et al. (2013a) because the reflections that I picked as the sequence boundary near the ACOW wells divides into two black negative reflections at the nearshore well logs. I decided to trace the middle of those two reflections (a white/positive) to be consistent over the loop correlation. Tracing the upper sequence boundary of Kw2a as a white/positive the seismic profiles appears to come in just above the m5.3 seismic reflection of Miller et al. (2013a) immediately landward of the Expedition 313 area, but tracing this white reflection into Sites M27 to M28 it appears to be closer to sequence boundary m5.2. However, the m5.3 sequence does not appear to be represented onshore (Fig. 22) and is very likely pinched-out or be truncated between at Expedition 313 site coreholes (Fig 21). Thus, my seismic tracings support correlation of sequence Kw2a with sequence m5.4. Future work should consider tracing the two black reflectors bracketing the white I traced from the ACOW1-2 wells to the Expedition 313 area.

5 Conclusion

This study comprises an interpretation of onshore and offshore late early Miocene sequences of New Jersey. For the onshore part of my study, I analyzed the CMZ and OV coreholes by integrating benthic biofacies, gamma ray logs, lithological changes, and observable stratal surfaces. For the offshore, I used gamma ray log data and inner to middle shelf multichannel seismic data to trace onshore sequence boundaries to their offshore equivalents.

Kw2a is interpreted as a composite sequence sensu Miller et al. (2001, 2005) at both OV and CMZ. A composite sequence is comprised of higher order, smaller scale sequences that are bounded by more localized sequence boundaries. These higher order sequences are generally associated with Milankovitch scale forcing on the sub 1 m.y. scale (e.g. Miller et al., 2013a). I reinterpreted composite Kw2a sequence in CMZ and OV coreholes and found enough physical evidence including thin shell beds, changes of stacking patterns, gamma ray log peaks, and mud peaks to divide the composite Kw2a sequence into higher order, individual sequences. In addition, Miller et al. (2000, 2005) and Kominz et al. (unpublished) provided Sr-isotope age estimates that support interpretation of Kw2a as a composite sequence (Fig. 22).

The lowermost higher order sequence is Kw2a1. This is the thickest sequence within the composite Kw2a sequence [630.7-549.5 ft (192.2-167.5 m) at CMZ and 640.4 ft - 531.2 ft (195.2-161.9 m) at OV]. Higher order sequence Kw2a1 contains a thin LST and relatively thick TST and HST at both CMZ and OV. Coarsening-upward LST's are comprised by two parts: devoid of foraminifera zone and the overlying zone deposited in inner neritic paleodepths (10-25 m). In both coreholes the TS is found where a possible progradational-stacking pattern (see "Discussion" section) shifts to a retrogradational stacking pattern. In addition, the TS marks the boundary where *Hanzawaia* spp. dominated inner neritic paleodepth (10-25 m) sediments deepen up to *Pseudononion* spp.-dominated inner to middle neritic paleodepth (25-50 m) sediments. The overlying TST comprise a generally fining and deepening upwards, mud-dominated succession. At the top of the TST, the MFS is marked by the highest abundances of *Uvigerina* spp. in both coreholes. The deepening upward, retrogradational stacking pattern changes to a progradational, shallowing upward succession as indicated by a shift from *Uvigerina* spp.-dominated biofacies (middle neritic; 75-100 m) to a *Hanzawaia* spp.-dominated biofacies (inner neritic; 10-25 m) up to the overlying higher sequence boundary.

A sequence boundary separates the Kw2a1 from the Kw2a2 higher order sequence at 549.5 ft (167.5 m) and 531.2 ft (161.9 m) at CMZ and OV, respectively. The sequence boundaries are interpreted from a minor gamma ray increase in association with a mud peak, rip up clasts and burrows in both coreholes. No LST is interpreted for the Kw2a2 higher sequence. On the other hand, a fining upwards TST unequivocally overlies the higher order sequence boundary up to the MFS where a the retrogradational TST stacking pattern changes to a coarsening upwards progradational HST. Semi-quantitative paleodepth estimates can't be made for higher order Kw2a2 sequence because it lacks foraminifera in the greater than 150 μm fraction in both coreholes.

A second higher order sequence boundary separates the Kw2a2 and Kw2a3 higher order sequences at 531.2 ft (161.9 m) and 502.2 ft (153.0 m), at CMZ and OV, respectively. The sequence boundary is interpreted from a minor gamma ray log increase, abrupt mud peak, and rip up clasts in both coreholes. The OV corehole provides enough benthic foraminifera, so I determined that the TST deepens from *Hanzawaia* spp. to *Pseudononion* spp. and shallows back to *Hanzawaia* spp. above the MFS in the HST. The CMZ corehole doesn't contain foraminifera to estimate paleodepths. Instead, I divided fining upwards TST and coarsening upwards MFS by lithological trend at 520.0 ft (158.5 m) where clay peak is reached and started to decrease.

For the onshore-offshore correlation section of my study, I projected and correlated gamma ray log data of the Kw2a composite sequence from onshore and nearshore wells to nearest seismic profiles, and traced its bounding reflections to IODP 313 coreholes site on New Jersey mid-shelf. This physical continuation proved that the onshore-determined composite Kw2a sequence boundaries correlate with composite sequences m5.4 reflection and might correlate m5.3 sequence boundaries (Fig. 21). However, pinched-out or truncated seismic beds cause ambiguity at Expedition 313 site coreholes (see "Discussion" section).

Miller et al. (2013a) proposed three higher order sequences (m5.4/1, m5.34, and 5.33) (Fig. 3) within composite sequence m5.4. Physical connection between onshore and offshore New Jersey sites shows the continuation of these major sequence boundaries from coastal plain through middle shelf. Three higher order sequences were both interpreted at onshore and offshore sites; however, no continuous tracing can be made for higher sequence boundaries because the reflections are below the resolution of seismic data and it is not possible to observe stratal relationships.

In general, this study suggests that preservation of LST is possible in Miocene onshore coreholes. The basal and top sequence boundaries of the composite Kw2a sequence are equivalent to m5.4 and m5.3 seismic reflections of Monteverde et al. (2008) and Miller et al. 2013a). Even though tracing can't be made for the higher sequence boundaries, three higher order sequences are found in onshore sites suggesting that onshore-offshore higher sequences boundaries could correlate (Kw2a1 and m5.4/1, Kw2a2 and m5.34, and Kw2a3 and m5.33).

6 References

Brown, L.F., and Fisher, W.L., 1977, Seismic-stratigraphic interpretation of depositional systems: Examples from Brazilian rift and pull-apart basins, *in* Payton, C.E., ed., Seismic stratigraphy—Applications to hydrocarbon exploration: American Association of Petroleum Geologists Memoir 26, p. 213–248.

Browning, J.V., Miller, K.G., McLaughlin, P.P., Kominz, M.A., Sugarman, P.J., Monteverde, D., Feigenson, M.D., and Hernàndez, J.C., 2006, Quantification of the effects of eustasy, subsidence, and sediment supply on Miocene sequences, Mid-Atlantic margin of the United States: Geological Society of America Bulletin, v. 118, p. 567–588, doi:10.1130/B25551.1.

Browning, J.V., Miller, K.G., Sugarman, P.J., Kominz, M.A., McLaughlin, P.P., and Kulpecz, A.A., 2008, 100 Myr record of sequences, sedimentary facies and sea-level change from Ocean Drilling Program onshore coreholes, U.S. Mid-Atlantic coastal plain: Basin Research, v. 20, p. 227–248, doi:10.1111/j.1365 - 2117.2008.00360.x.

Browning, J.V., Miller, K.G., Sugarman, P.J., Barron, J., McCarthy, F.M.G., Kulhanek, D.K., Katz, M.E., and Feigenson, M.D., 2013, Chronology of Eocene–Miocene sequences on the New Jersey shallow shelf: Implications for regional, interregional, and global correlations: Geosphere, doi:10.1130/GES00857.1.

Catuneau, O., 2006, Principles of sequence stratigraphy, Elsevier, New York, 375 p.

Christie-Blick, N., Mountain, G.S., and Miller, K.G., 1990, Seismic stratigraphic record of sea-level change, in Geophysics Study Committee, National Research Council, Sea-level change: National Academy of Sciences Studies in Geophysics: Washington, D.C., National Academy Press, p. 116–140.

Coe, A.L., ed., 2003, The sedimentary record of sea level change: Cambridge, Cambridge University Press, 288 p.

de Verteuil, L., Palynological delineation and regional correlation of lower through upper Miocene sequences in the Cape May and Atlantic City boreholes, New Jersey coastal plain, *Proc. Ocean Drill. Program, Sci. Results, 150X,* 129–145, 1997.

Galloway, W.E., 1989, Genetic stratigraphic sequences in basin analysis I: Architecture and genesis of flooding- surface bounded depositional units: American Association of Petroleum Geologists, Bulletin, v. 73, p. 125–142.

Greenlee, S.M., Moore, T.C., 1988, Recognition and interpretation of depositional sequences and calculations of sea level changes from stratigraphic data-offshore New Jersey and Alabama Tertiary, An Integrated Approach, Society of Economic Paleontologists and Mineralogists, Special Publication (Eds. Wilgus, C.K., Hastings, B.S., Kendall, C.G.St.C., Posamentier, H.W., Ross, C.A., Van Wagoner, J.C., Sea Level Changes), v. 42, p. 329-353.

Greenlee, S.M., Devlin, W.J., Miller, K.G., Mountain, G.S., and Flemings, P.B., 1992, Integrated sequence stratigraphy of Neogene deposits, New Jersey continental shelf and slope: comparison with the Exxon model, Geological Society of America Bulletin, v. 104, p. 1403-1411.

Hathaway, J.C., Poag, C.W., Valentine, P.C., Miller, R.E., Schultz. D.M., Manheim, R.T., Kohout, F.A., Bothner, M.H., and Sangrey, D.A., 1979, U.S. Geological Sur- vey core drilling on the Atlantic shelf: Science, v. 206, p. 515–527.

Katz, M.E., Miller, K.G., and Mountain, G.S., 2003a, Bio- facies and lithofacies evidence for paleoenvironmental interpretations of upper Neogene sequences on the New Jersey continental shelf (ODP Leg 174A), *in* Olson, H.C., and Leckie, R.M., eds., Micropaleontologic proxies for sea-level change and stratigraphic discontinuities: SEPM (Society for Sedimentary Geology) Special Publication 75, p. 131–146, doi:10.2110/pec.03.75.0131

Katz, M.E., Browning, J.V., Miller, K.G., Monteverde, D., Mountain, G.S., and Williams, R.H., 2013, Paleobathymetry and sequence stratigraphic interpretations from benthic foraminifera: Insights on New Jersey shelf architecture, IODP Expedition 313: Geosphere, doi:10.1130/GES00872.1.

Kominz, M.A., and Pekar, S.F., 2001, Oligocene eustasy from two-dimensional sequence stratigraphic backstripping: Geological Society of America Bulletin, v. 113, p. 291–304, doi: 10.1130/0016-7606(2001)113<0291: OEFTDS>2.0.CO;2.

Loutit, T.S., Hardenbol, J., Vail, P.R., and Baum, G.R., 1988, Condensed section: The key to age determination and correlation of continental margin sequences, *in* Wilgus, C.K., et al., eds., Sea-level changes: An integrated approach: Society of Economic Paleontologists and Mineralogists Special Publication 42, p. 183–213, doi:10.2110/pec.88.01.0183.

Miall, A.D., 1991, Stratigraphic sequences and their chronostratigraphic correlation: Journal of Sedimentary Petrology, v. 61, p. 497–505.

Miller, K.G., Liu, C., Browning, J.V., Pekar, S.F., Sugarman, P.J., Van Fossen, M.C., Mullikin, L., Queen, D., Feigenson, M.D., Aubry, M.P., Burckle, L.D., Powars, D., and Heibel, T., 1996, Cape May site report, Proceedings of the Ocean Drilling Program, Initial Reports, Leg 150X (supplement): College Station, TX

Miller, K.G., Mountain, G.S., Leg 150 Shipboard Party, and Members of the New Jersey Coastal Plain Drilling Project, 1996, Drilling and dating New Jersey Oligocene–Miocene sequences: Ice volume, global sea level, and Exxon records: Science, v. 271, p. 1092–1095, doi:10.1126/science.271.5252.1092.

Miller, K.G., 1997, Coastal plain drilling and the New Jersey Sea-level Transect, Proceedings of the Ocean Drilling Program, Initial Reports, Leg 150X (supplement): College Station, TX, Ocean Drilling Program, p.3-12.

Miller, K.G., Rufolo, S., Sugarman, P.J., Pekar, S.F., Browning, J.V., and Gwynn, D.W., 1997, Early to middle Miocene sequences, systems tracts, and benthic foraminiferal biofacies, New Jersey coastal plain, *in* Miller, K.G., and Snyder, S.W., eds., Proceedings of the Ocean Drilling Program, Scientific Results, Leg 150X: College Station, Texas, Ocean Drilling Program, p. 169 186.

Miller, K.G., Mountain, G.S., Browning, J.V., Kominz, M., Sugarman, P.J., Christie-Blick, N., Katz, M.E., and Wright, J.D., 1998, Cenozoic global sea-level, sequences, and the New Jersey transect: Results from coastal plain and slope drilling: Reviews of Geophysics, v. 36, p. 569–601, doi:10.1029/98RG01624.

Miller, K.G., Browning, J.V., Mountain, G.S., Bassetti, M.A., Monteverde, D., Katz, M.E., Inwood, J., Lofi, J., and Proust, J.N., 2013, Sequence boundaries are impedance contrasts: Core-seismic-log integration of Oligocene–Miocene sequences, New Jersey shallow shelf: Geosphere, v. 9, doi:10.1130/GES00858.1.

Miller, K.G., and 13 others, 2013a, Testing sequence stratigraphic models by drilling Miocene foresets on the New Jersey shallow shelf: Geosphere, v. 9, doi:10.1130/GES00884.1.

Miller, K.G., Browning, J.V., Mountain, G.S., Bassetti, M.A., Monteverde, D., Katz, M.E., Inwood, J., Lofi, J., and Proust, J.N., 2013b, Sequence boundaries are impedance contrasts: Core-seismic-log integration of Oligocene–Miocene sequences, New Jersey shallow shelf: Geosphere, v. 9, doi:10.1130/GES00858.1.

Mitchum, R.M., Jr., Vail, P.R., and Thompson, S., III, 1977, Seismic stratigraphy and global changes of sea level; Part 2, The depositional sequence as a basic unit for stratigraphic analysis, *in* Payton, C.E., ed., Seismic stratigraphy; applications to hydrocarbon exploration: American Association of Petroleum Geologists Memoir 26, p. 53–62.

Monteverde, D.H., Miller, K.G., And Mountain, G.S., 2000, Correlation of offshore seismic profiles with onshore New Jersey Miocene sediments: Sedimentary Geology, v. 134, p. 111– 128.

Monteverde, D.H., 2008, Sequence stratigraphic analysis of early and middle Miocene shelf progradation along the New Jersey margin [Ph.D. thesis]: New Brunswick, Rutgers University, 247 p.

Monteverde, D.H., Mountain, G.S., and Miller, K.G., 2008, Early Miocene sequence development across the New Jersey margin: Basin Research, v. 20, p. 249–267, doi: 10.1111/j.1365-2117.2008.00351.x.

Mountain, G.S., Miller, K.G., Blum, P., et al., 1994, Proceedings of the Ocean Drilling Program, Initial Reports, Leg 150X: College Station, TX, Ocean Drilling Program, 885 p.

Mountain, G., Proust, J.N., McInroy, D., Cotterill, C., and the Expedition 313 Scientists, 2010, Proc. IODP, 313: Tokyo (Integrated Ocean Drilling Program Management International, Inc.). doi:10.2204/ iodp.proc.313.

Neal, J., Abreu, V., 2009, Sequence stratigraphy hierarchy and the accommodation succession method, Geology, 37;779-782.

Pazzaglia, F.J., 1993, Stratigraphy, petrography and correlation of late Cenozoic middle Atlantic Coastal Plain deposits: Implications for late-stage passive-margin geologic evolution, Geological Society of America, Bulletin, v. 105, p. 1617-1634.

Plint, A.G., and Nummedal, D., 2000, The falling stage systems tract: Recognition and importance in sequence stratigraphic analysis, *in* Hunt, D., and Gawthorpe, R.L., eds., Sedimentary responses to forced regression: Geological Society of London Special Publication 172, p. 1–17, doi:10.1144/GSL.SP.2000.172.01.01.

Pekar, S.F., Christie-Blick, N., Kominz, M.A., and Miller, K.G., 2001, Evaluating the stratigraphic response to eustasy from Oligocene strata in New Jersey: Geol- ogy, v. 29, p. 55–58, doi:10.1130/0091-7613(2001)029 <0055:ETSRTE>2.0.CO;2.

Posamentier, H.W., and Vail, P.R., 1988, Eustatic controls on clastic deposition II—Sequence and systems tract models, *in* Wilgus, C.K., et al., eds., Sea level changes: An integrated approach: Society of Economic Paleontologists and Mineralogists Special Publication 42, p. 125–154, doi:10.2110/pec.88.01.0125.

Poag, C.W., 1978, Stratigraphy of the Atlantic continental shelf and slope of the United States. Ann. Rev. Earth Planet. Sci., v. 6, p. 251-280.

Poag, C. W., 1979, Stratigraphy and Depositional Environments of Baltimore Canyon Trough, Bull. Am. Assoc. Pet. Geol. 63, 1452–146

Poag, C.W., and Sevon, W.D., 1989, A record of Appalachian denudation in post-rift Mesozoic and Cenozoic sedimentary deposits of the US middle Atlantic continental margin, Geomorphology, v. 2, p. 119-157.

Posamentier, H.W., Jervey, M.T., and Vail, P.R., 1988, Eustatic controls on clastic deposition I—Conceptual framework, *in* Wilgus, C.K., et al., eds., Sea-level changes: An integrated approach: Society of Economic Paleontologists and Mineralogists Special Publication 42, p. 109–124, doi:10.2110/pec.88.01.0109.

Schlee, J.S., 1981, Seismic stratigraphy of Baltimore Canyon Trough: American Association of Petroleum Geologists Bulletin, v. 65, p. 26–53.

Snyder, S.W., Waters, V.J., and Moore, T.L., 1988, Benthic foraminifera and paleoecology of Miocene Pungo River Formation sediments in Onslow Bay, North Carolina continental shelf, *in* Snyder, S.W., ed., Micropaleontology of Miocene sediments in the shallow subsurface of Onslow Bay, North Carolina continental shelf: Cushman Foundation for Foraminiferal Research Special Publication 25, p. 76–95.

Sugarman, P.J., Miller, K.G., Owens, J.P., and Feigenson, M.D., 1993, Strontium-isotope and sequence stratigraphy of the Miocene Kirkwood Formation, southern New Jersey: Geological Society of America Bulletin, v. 105, p. 423–436, doi:10.1130/0016-7606(1993)105<0423: SIASSO>2.3.CO;2.

Vail, P. R. and Wornardt, W. W. (1990): Well log seismic Sequence stratigraphy: An integrated tool for the 90's: gulf coast section of Society of Economic Paleontologist and Mining Foundation, Eleventh Annual Research program and extended abstract, pp. 379–388.

Van der Zwaan, G.J., Duijnstee, I.A.P., den Dulk, M., Ernst, S.R., Jannink, N.T., Kouwenhoven, T.J., 1999. Benthic foraminifers: proxies or problems? A review of paleocological concepts. Earth-Sci. Rev. 46: 213–236.

Van Wagoner, J.C., Posamentier, H.W., Mitchum, R.M., Vail, P.R., Sarg, J.F., Loutit, T.S., and Hardenbol, J., 1988, An overview of the fundamentals of sequence stratigraphy and key definitions, *in* Wilgus, C.K., et al., eds., Sea-level changes: An integrated approach: Society of Economic Paleontologists and Mineralogists Special Publication 42, p. 39–45, doi:10.2110/pec.88.01.0039.

Van Wagoner, J.C., Mitchum, R.M., Campion, K.M., and Rahmanian, V.D., 1990, Siliciclastic sequence stratigraphy in well logs, cores, and outcrops: Concepts for high-resolution correlation of time and facies: American Association of Petroleum Geologists Methods in Exploration Series 7, 55

7 Figures

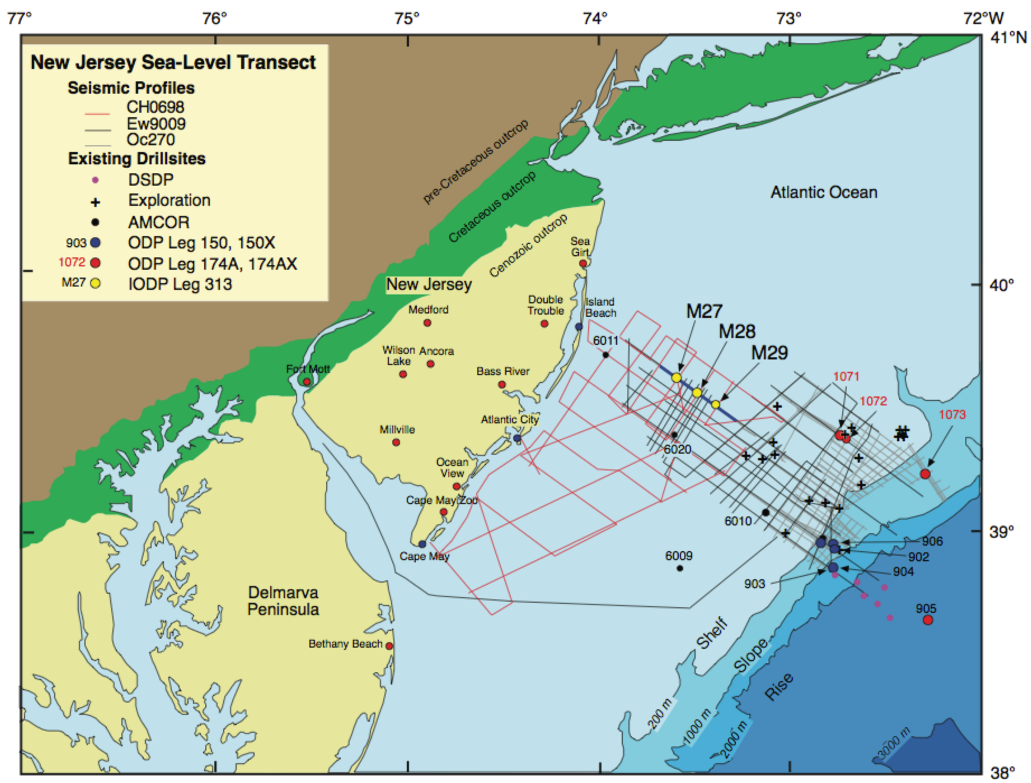

Figure 1: Generalized location map of New Jersey Transect (Miller et al., 2013a)

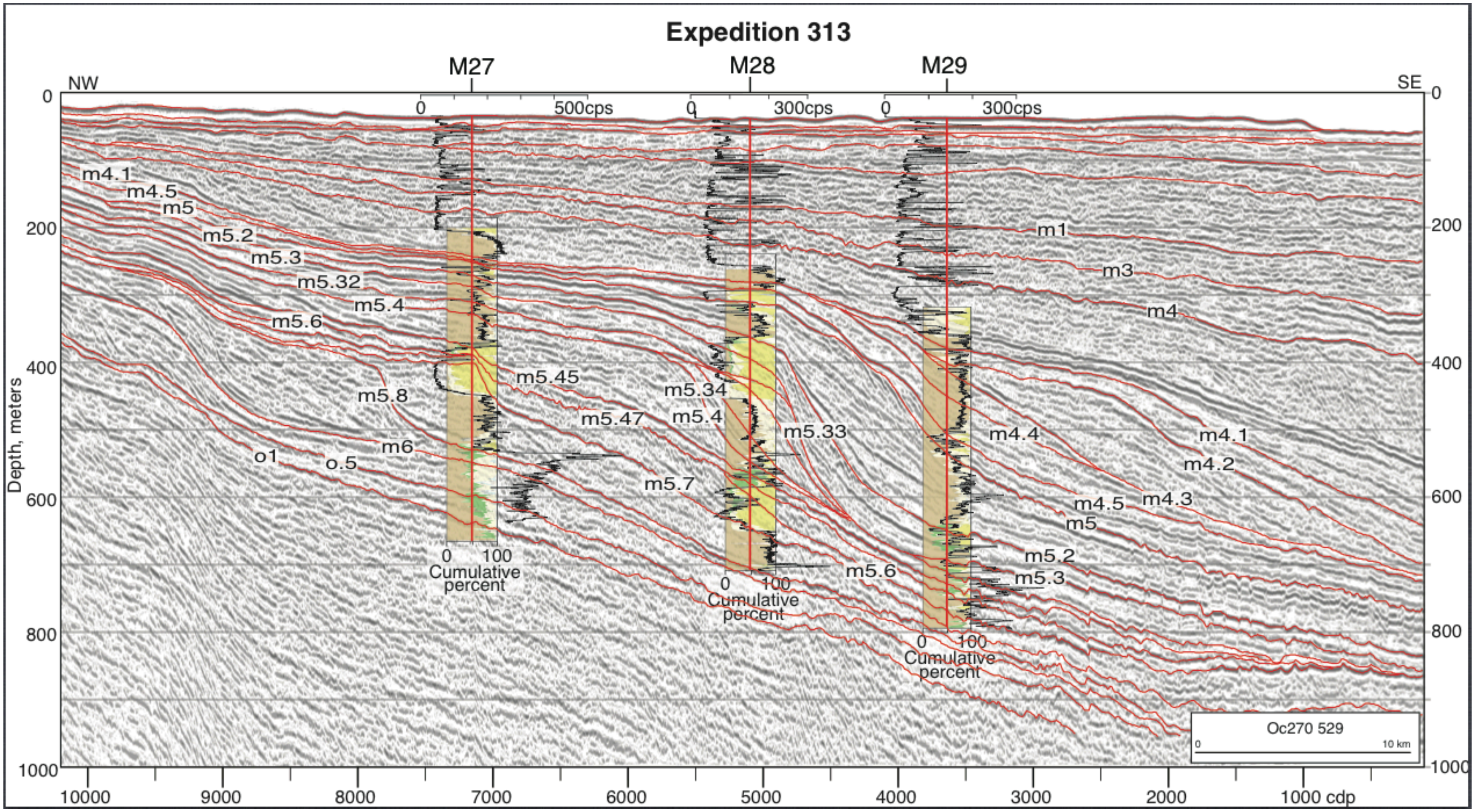

Figure 2: Sequence boundaries (Late Oligocene to Pleistocene) of offshore New Jersey at Expedition 313 Site (Miller et al., 2013a)

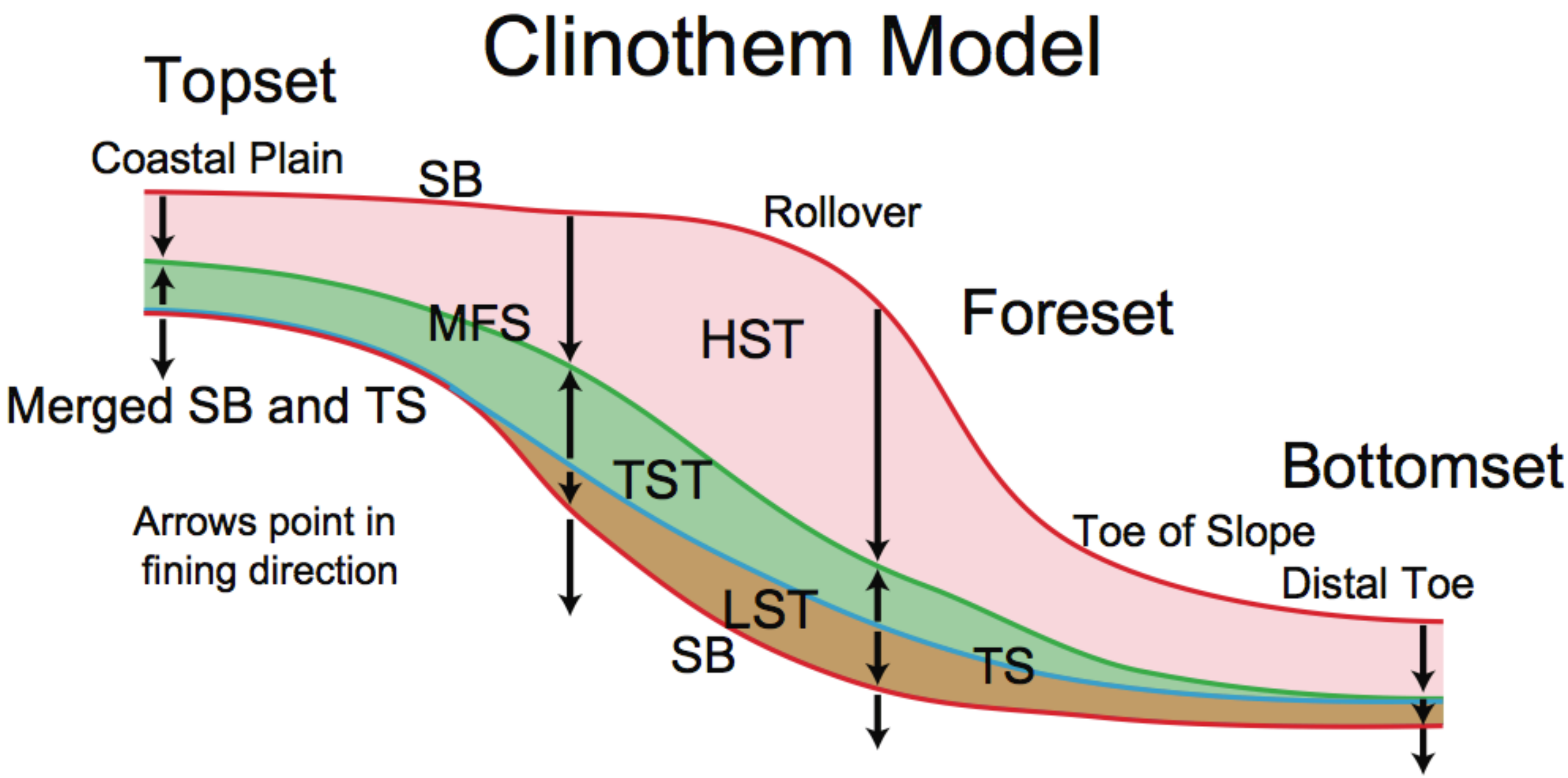

Figure 3: Generalized sequence stratigraphy of a clinoform (modified from Miller et al., 2013a)

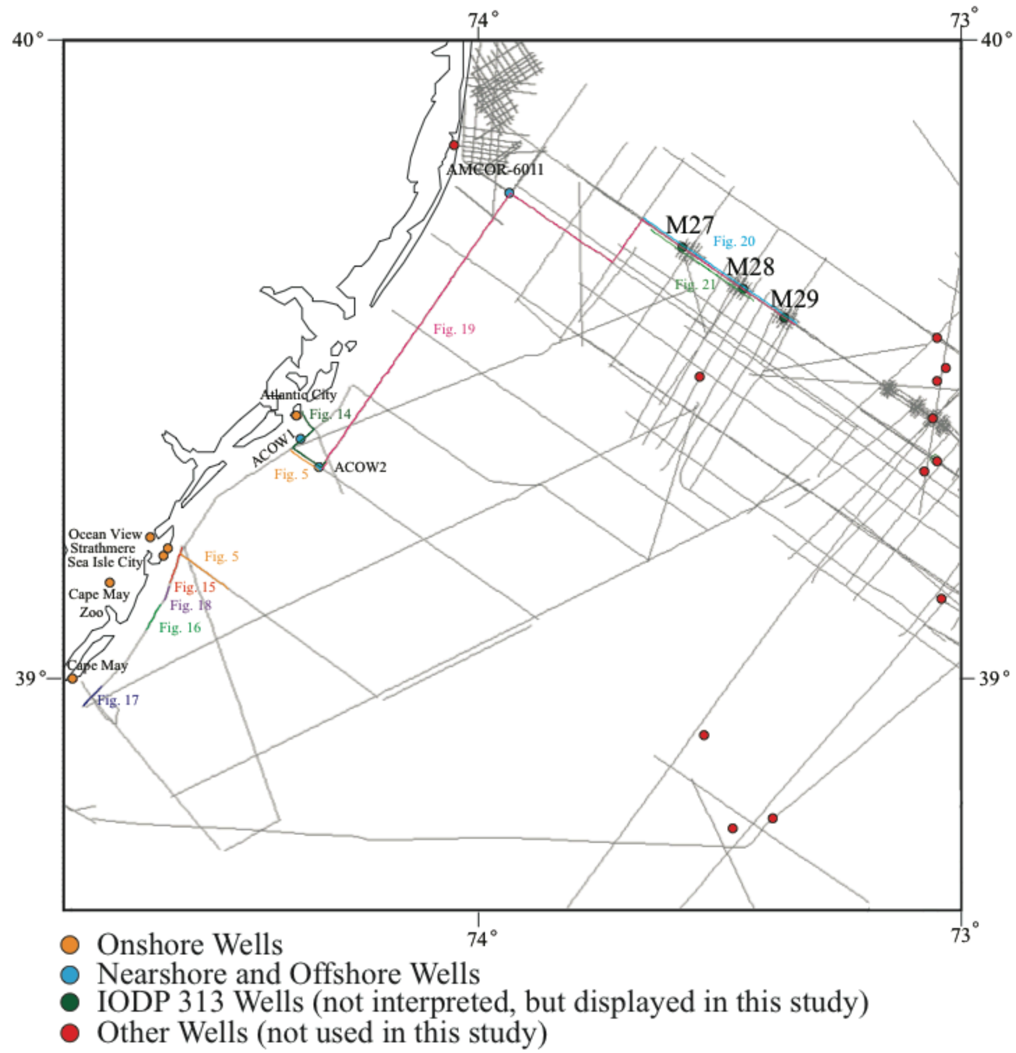

Figure 4: Well log locations and figure numbers of seismic profiles in this study

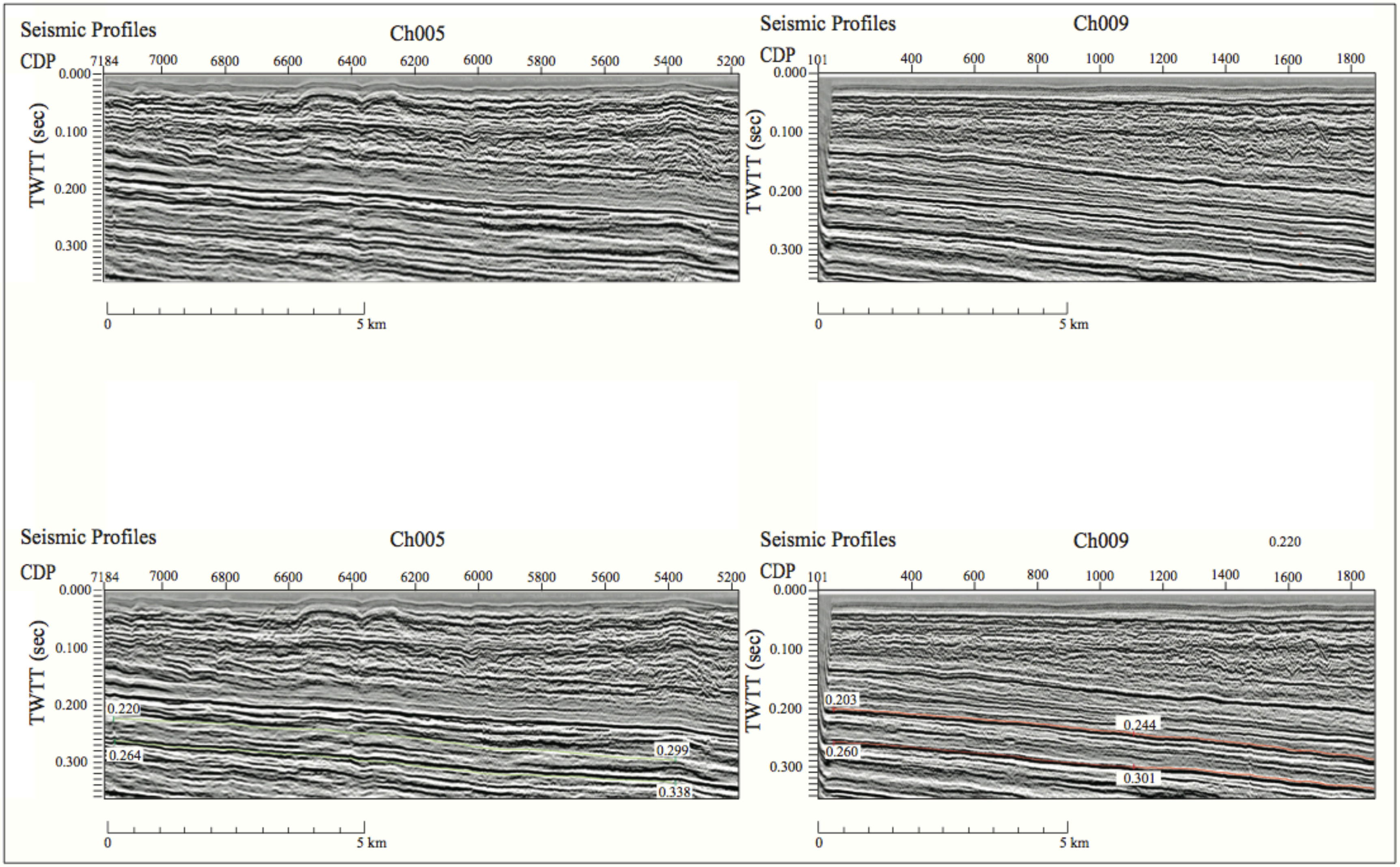

Figure 5: Uninterpreted (above) and interpreted (below) seismic profiles of CH0698 5 and 9 seismic profiles show uniform thickness and gradient change over inner shelf. The calculation is provided in Table 2.

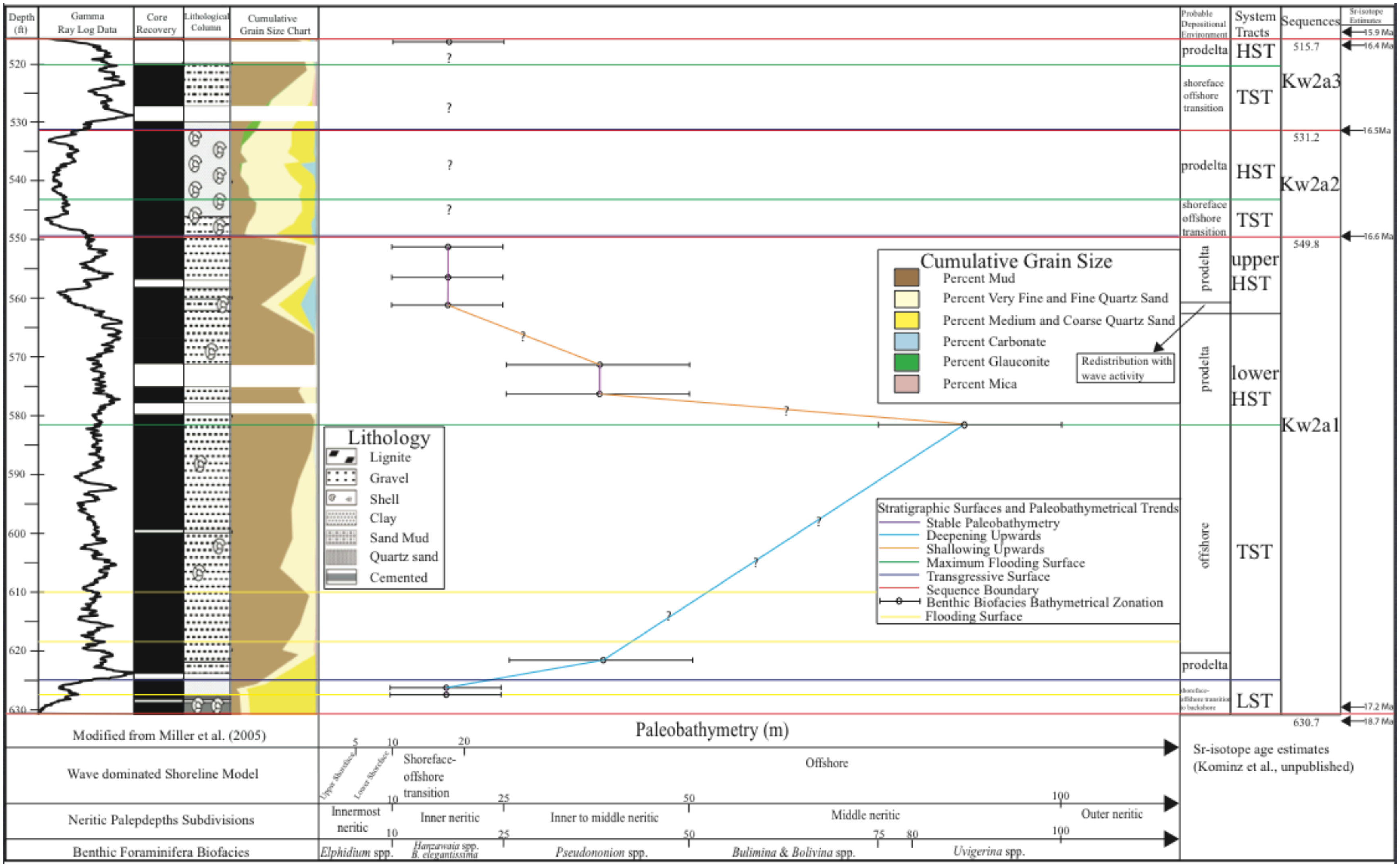

Figure 6: Integration of lithology, gamma ray log character, grain size, and semi quantitative benthic foraminifera paleobathymetrical curve of Cape May Zoo composite Kw2a sequence corehole data in a sequence stratigraphic framework

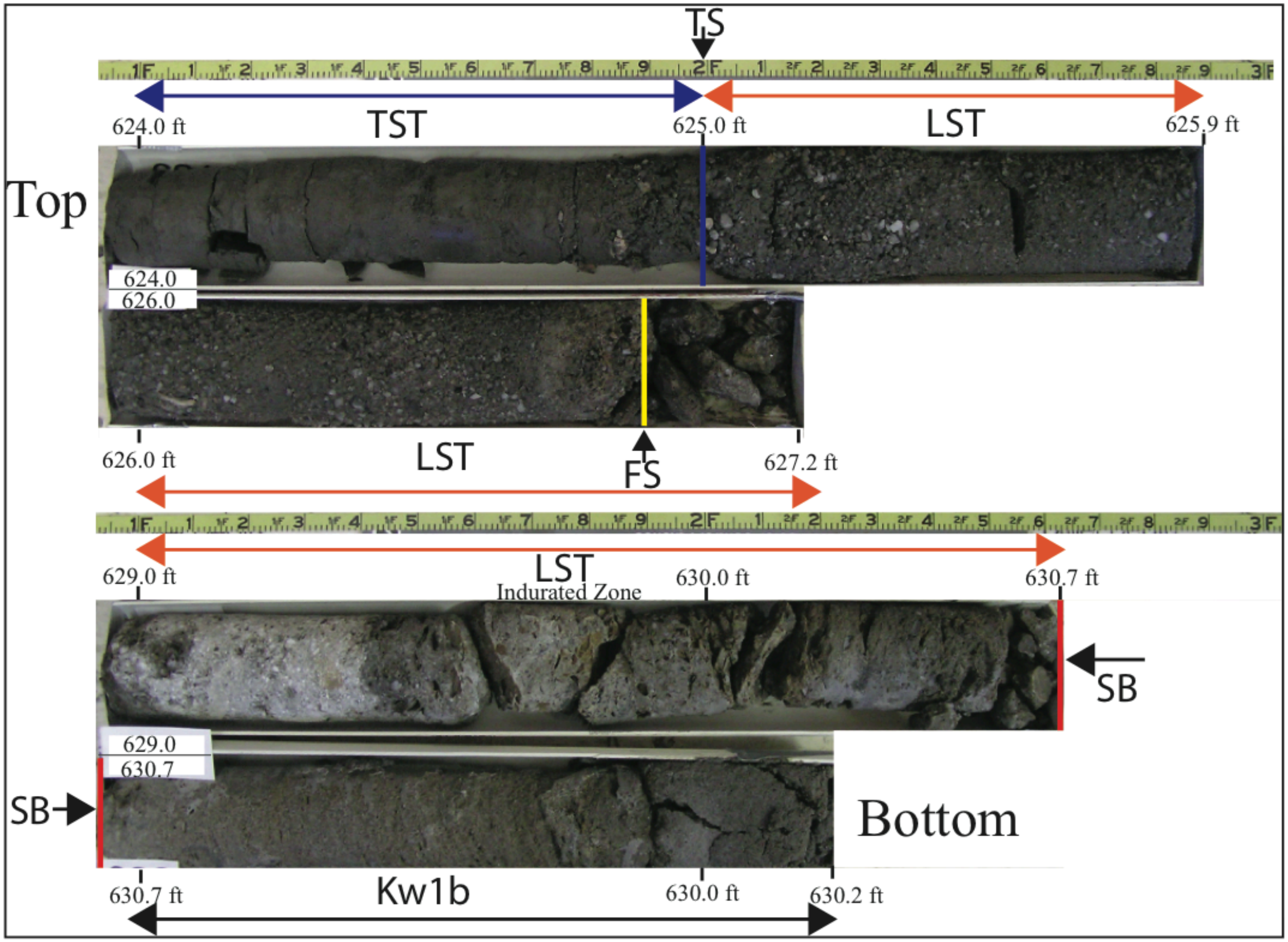

Figure 7: The proposed LST of higher order Kw2a1 sequence of Cape May Zoo corehole including stratal surfaces (SB, FS, and TS) and system tracts

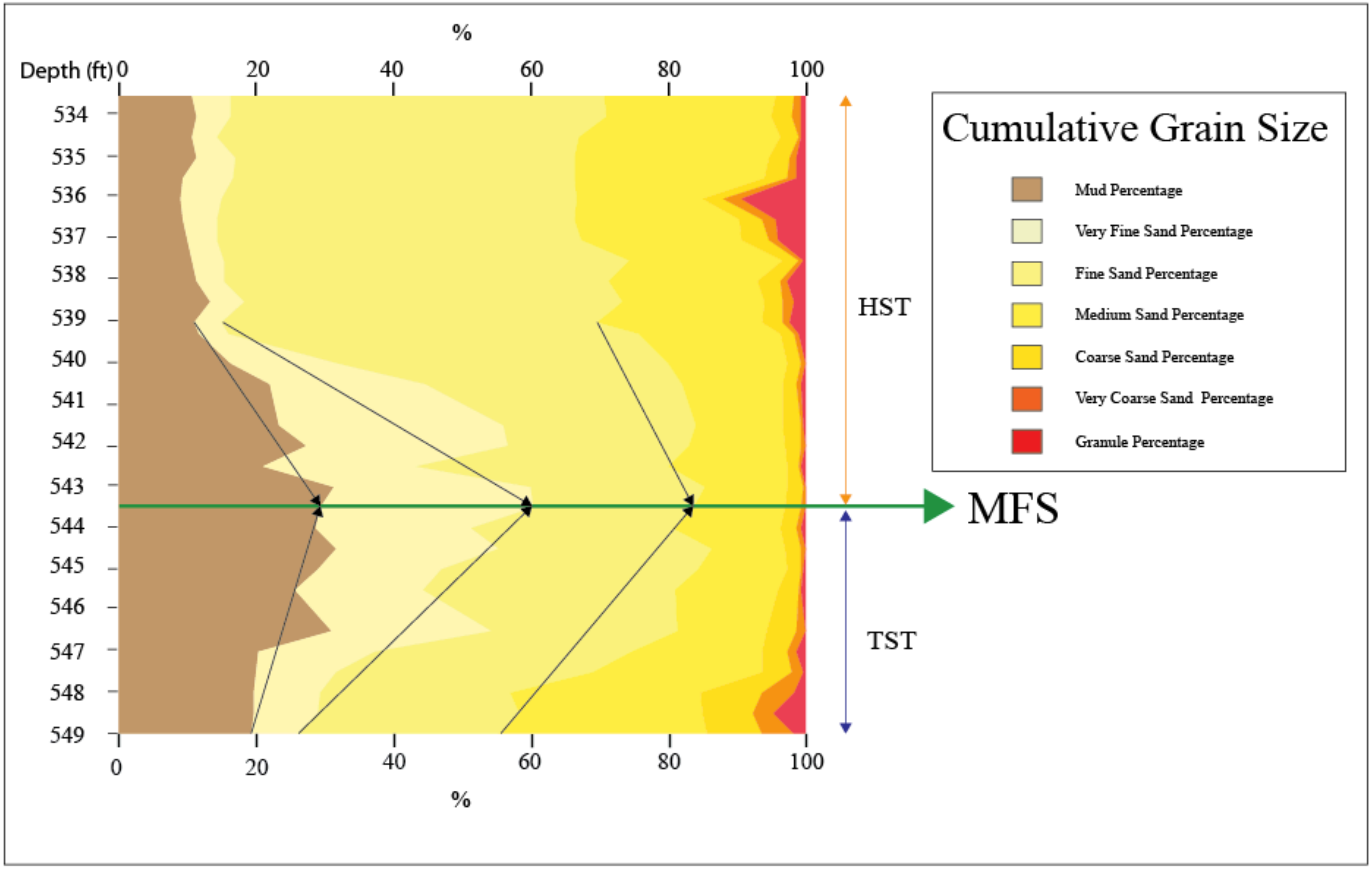

Figure 8: Grain size analysis of higher order Kw2a2 sequence in Cape May Zoo corehole shows MFS. Black arrows are showing fining direction.

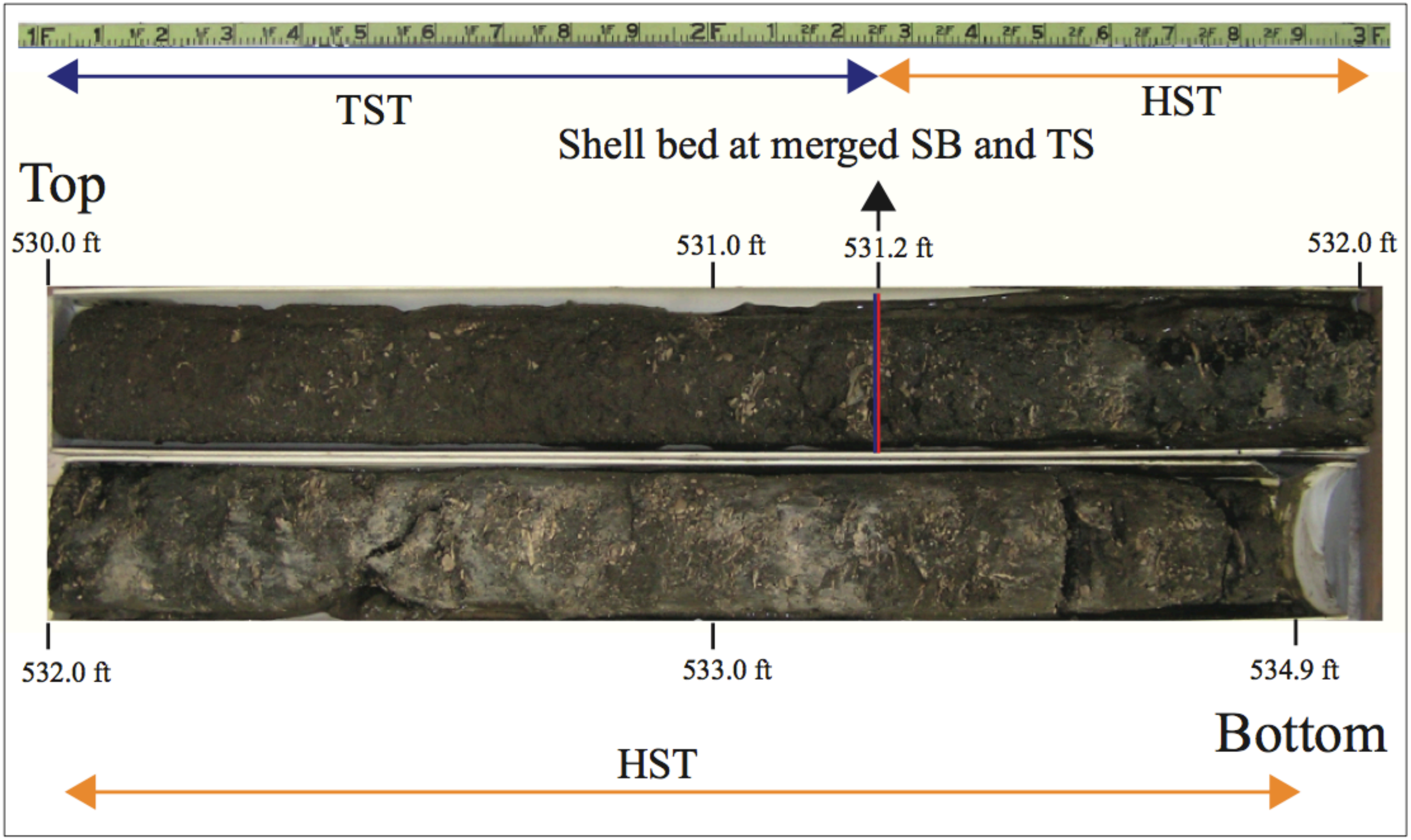

Figure 9: The merged sequence boundary and transgressive surface that separates higher order sequence of Kw2a2 from Kw2a3 at 531.2 ft in Cape May Zoo corehole.

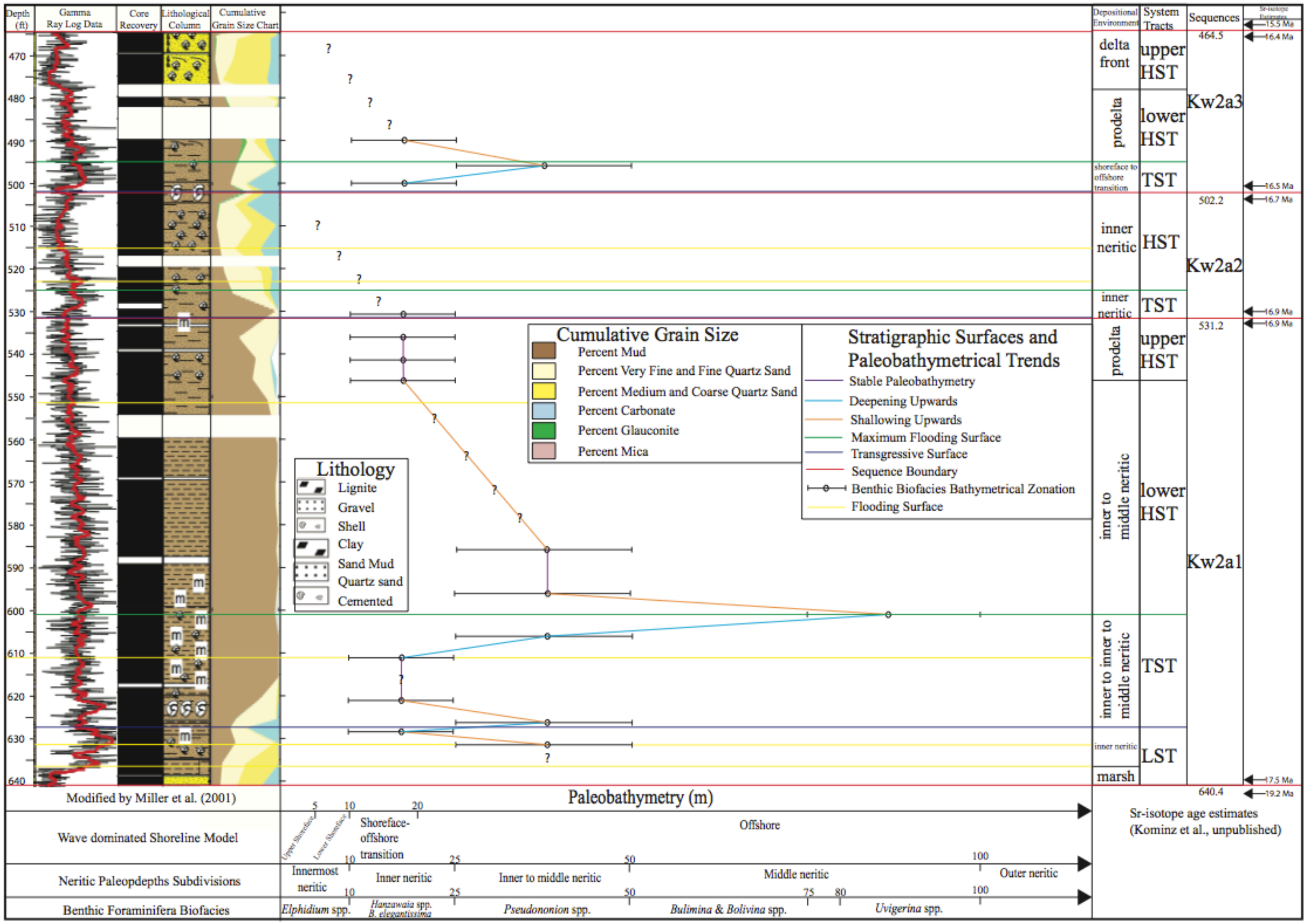

Figure 10: Integration of lithology, gamma ray log character, grain size, and semi quantitative benthic foraminifera paleobathymetrical curve of Ocean View composite Kw2a sequence corehole data in a paleodepositional and sequence stratigraphic framework

Figure 11: At 627 ft pale light gray indurated calcareous claystone marks the boundary between dark colored laminated shoreface-offshore transitional (inner neritic) mudstone and offshore, inner to middle neritic transgressive system tract facies of higher order Kw2a1 sequence in Ocean View corehole.

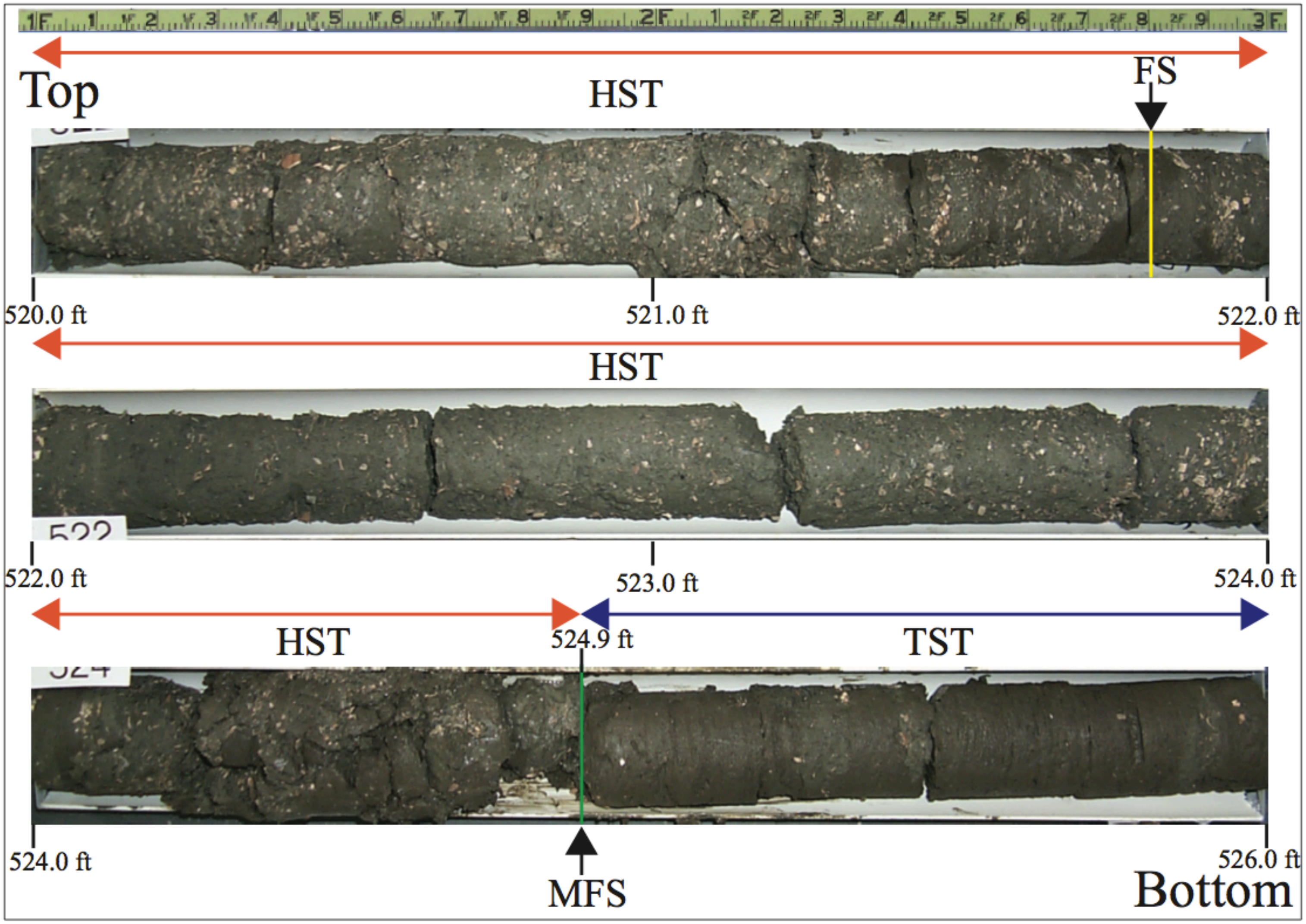

Figure 12: In Ocean View corehole, MFS marks the boundary between finely laminated inner neritic mud dominated TST facies and shelly, blocky fine to medium sand dominated HST facies. A flooding surface occurs within HST.

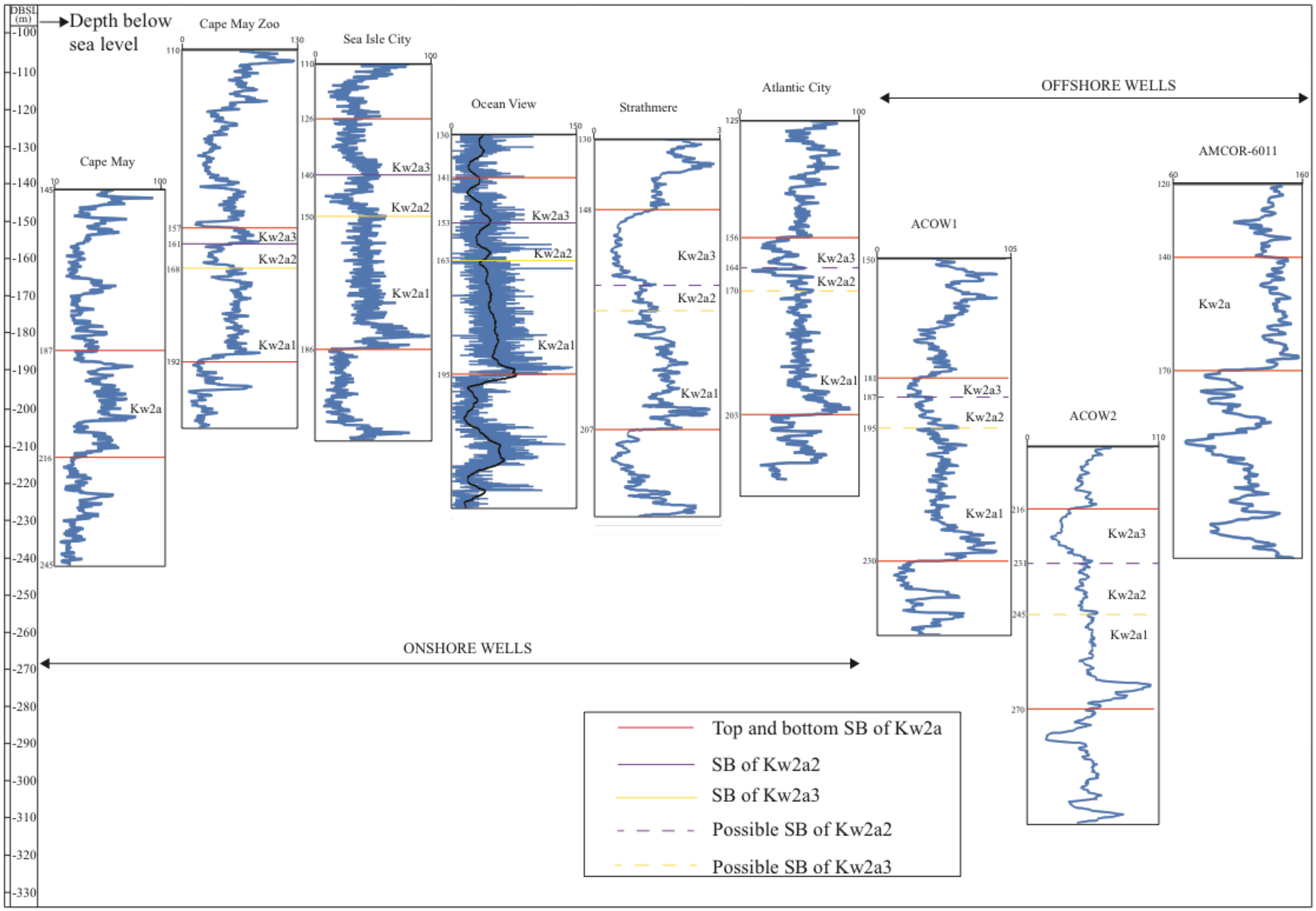

Figure 13: Gamma ray log correlation over Leg 150X, 174AX onshore well logs and U.S.G.S. onshore and offshore well logs regardless of seismic data. Higher order sequences Kw2a1, Kw2a2, and Kw2a3 were interpreted in CMZ, SIC, OV, AC, and ACOW1.

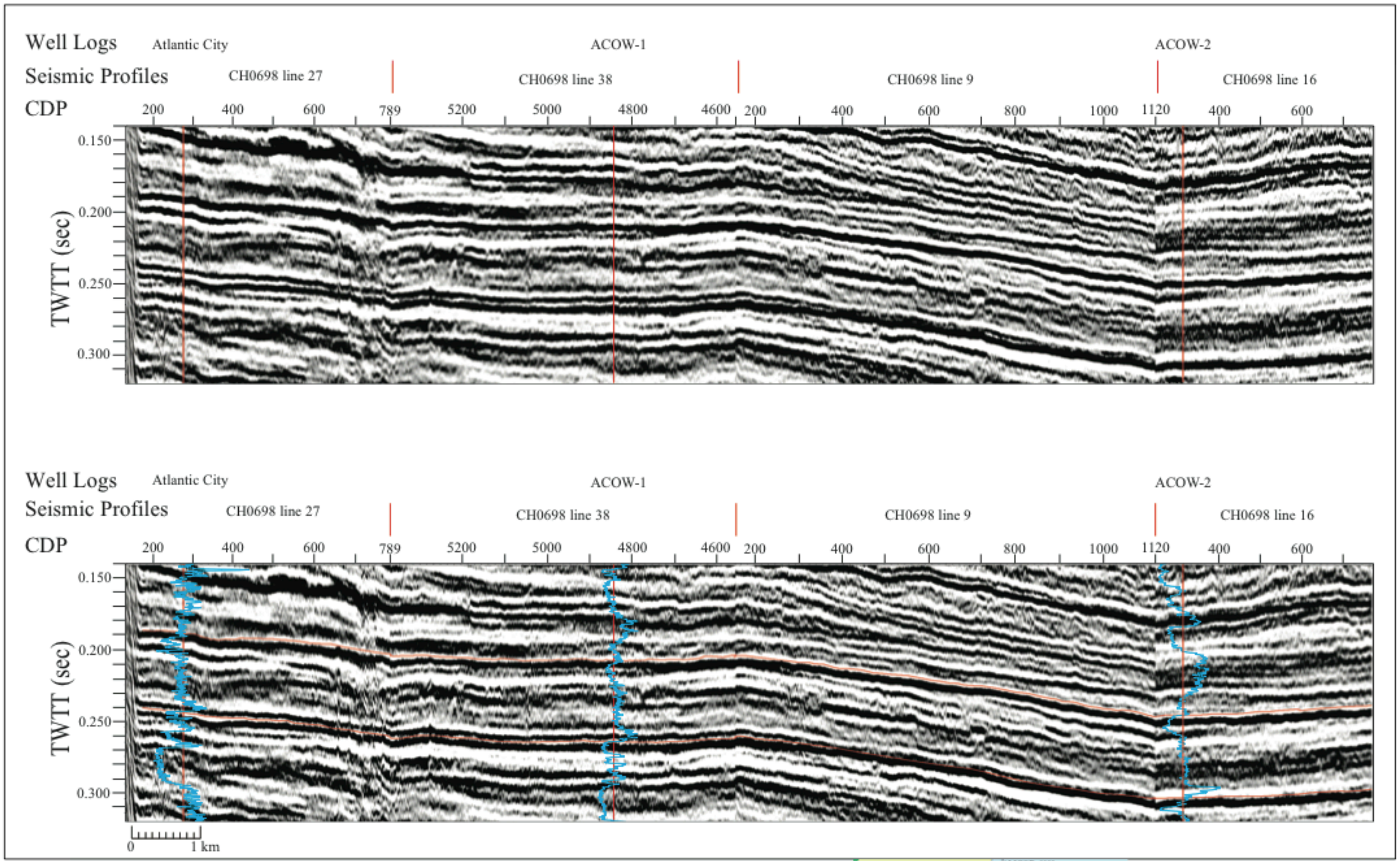

Figure 14: Loop correlation over CH0698 27, 38, 9, and 16 seismic profiles shows the continuity of Kw2a gamma ray log characters and equivalent seismic reflection of top and basal composite Kw2a sequence boundaries.

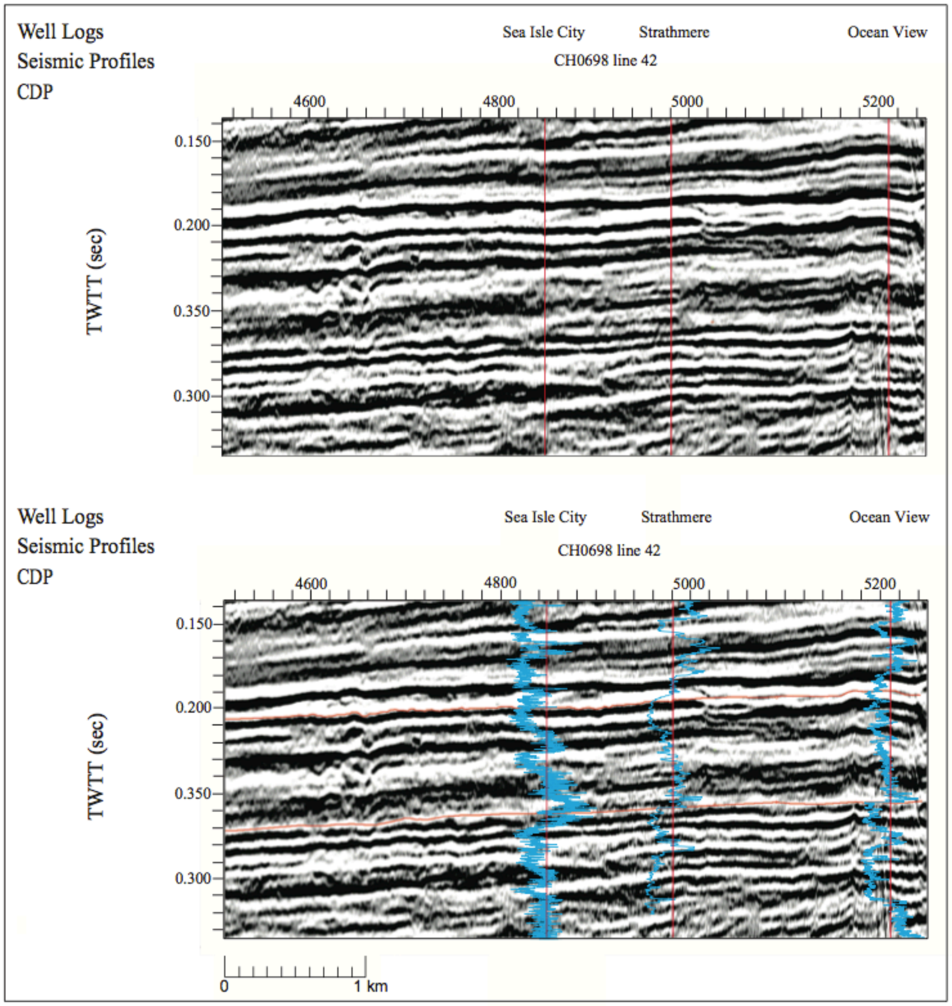

Figure 15: Gamma ray log correlation is projected onto CH0698 42 seismic profile and the sequence boundaries that traced from CH0698 38 seismic profile were loop correlated with previously proposed gamma ray log data peaks for top and basal sequence boundaries for composite Kw2a sequence.

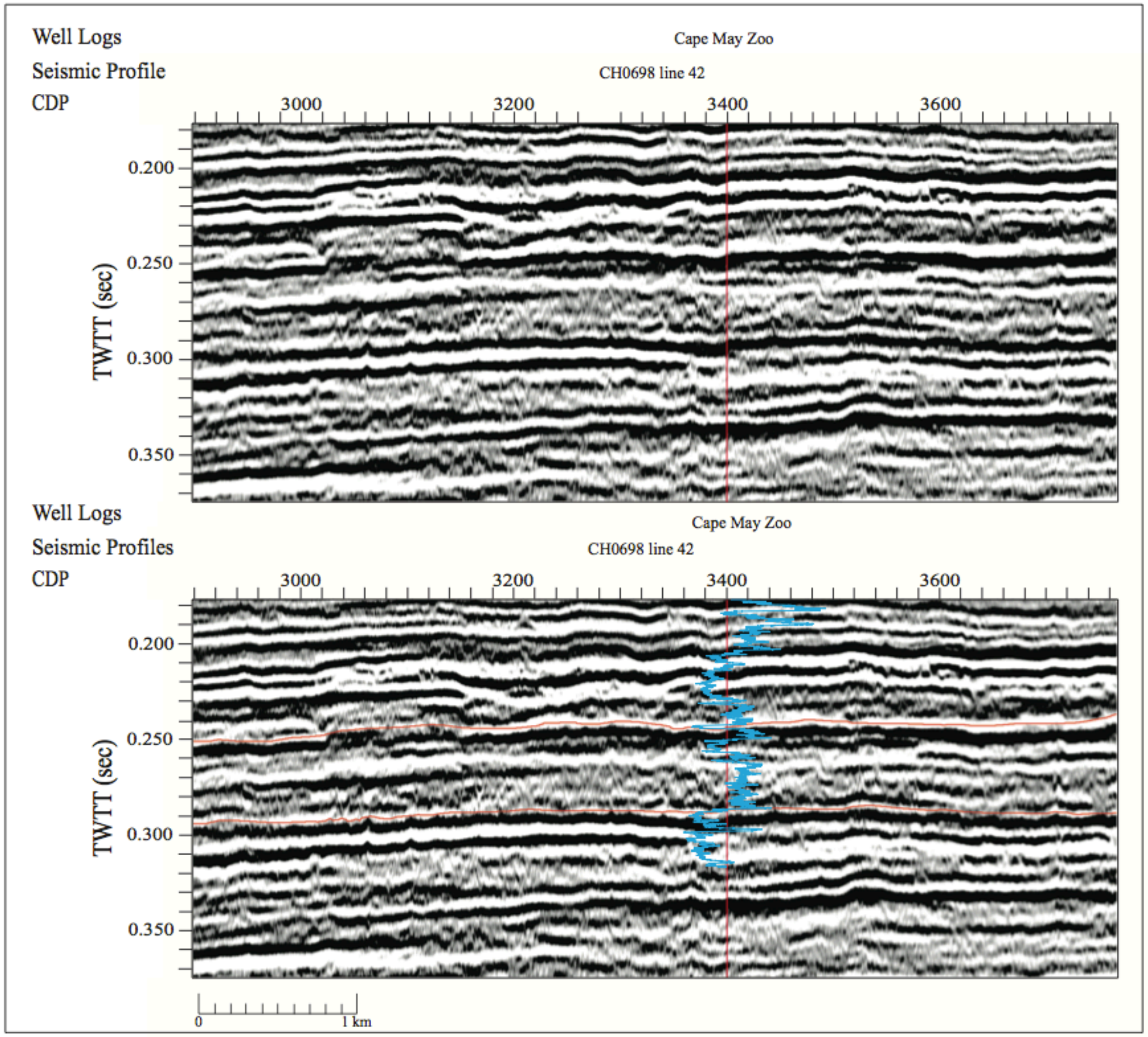

Figure 16: Cape May Zoo gamma ray log data directly projected onto CH0698 42 line. Seismic reflections represent top and basal sequence boundaries of composite Kw2a sequence traced from OV, SIC, and Strathmere well logs.

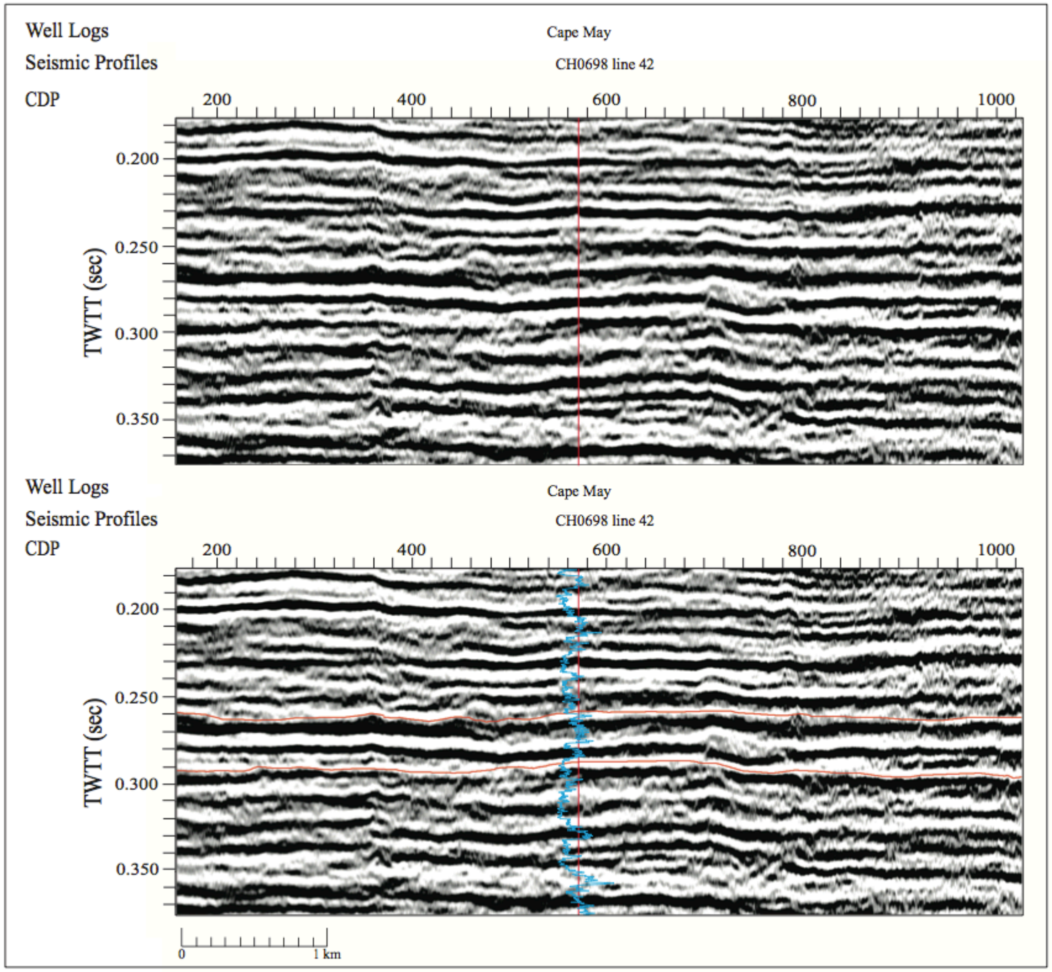

Figure 17: Cape May gamma ray log data directly projected onto CH0698 42 line. Seismic reflections represent top and basal sequence boundaries of composite Kw2a sequence.

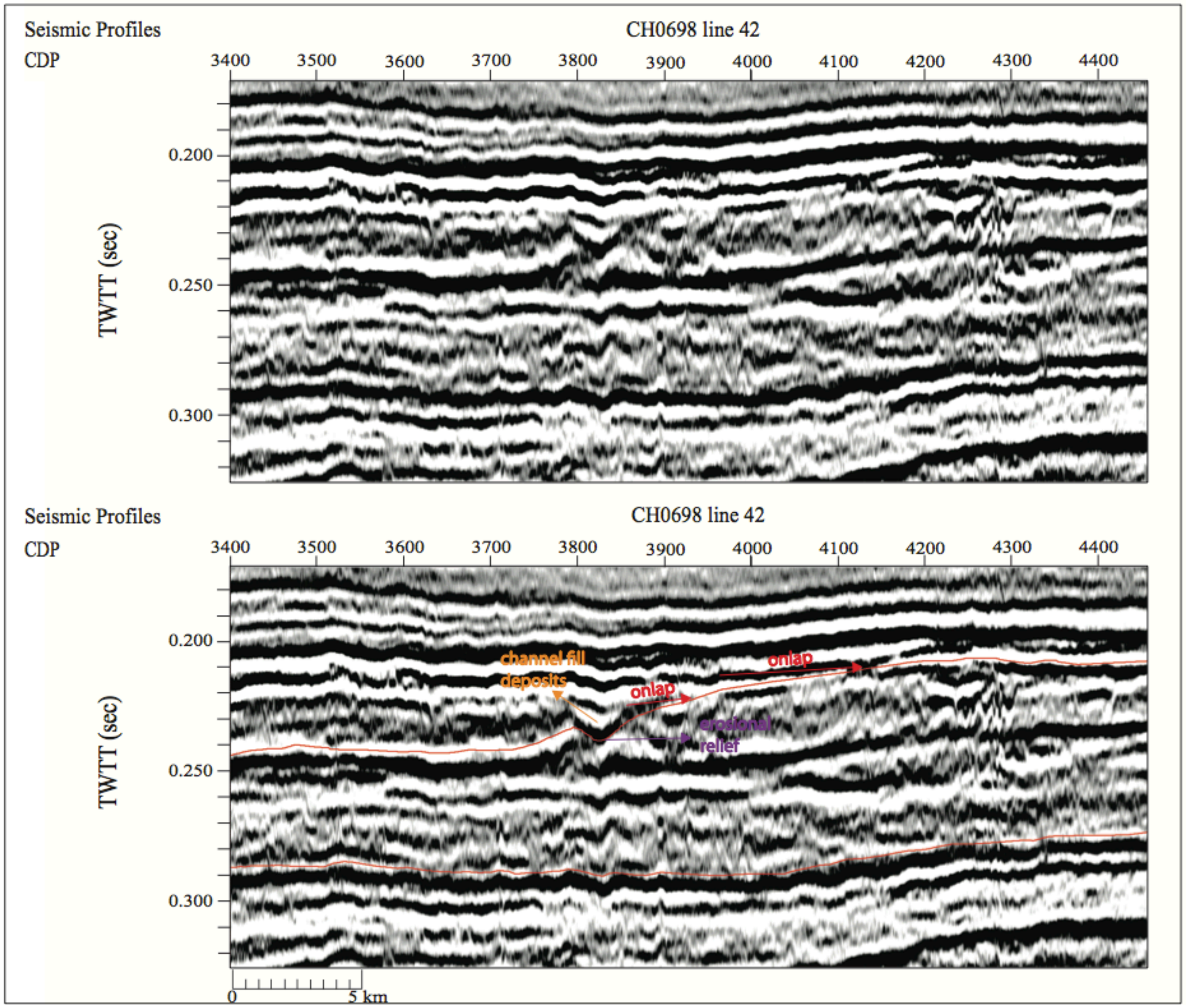

Figure 18: Younger strata onlap onto the upper sequence boundary of composite Kw2a sequence. An erosional relief, which is in connection with the overlying sequence boundary, is filled with younger (upper sequence) sediment

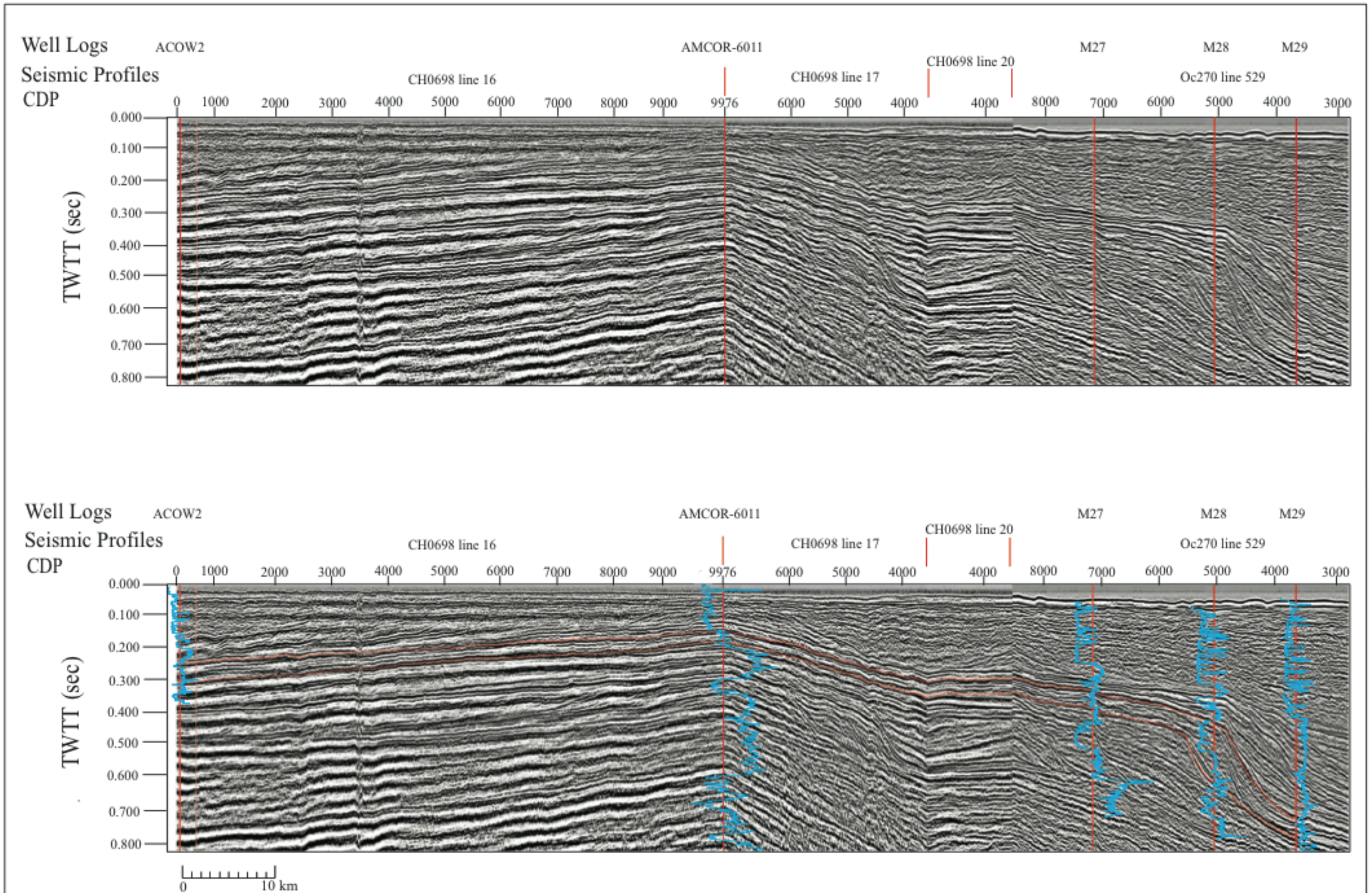

Figure 19: Loop correlated profile shows the physical connection between inner ACOW2 and middle shelf M27, M28, and M29 well logs in 4 different seismic profiles. The red colored reflection shows physical connection of onshore Kw2a sequence boundaries and m5.4 and m5.2 of sensu (Monteverde et al., 2008; and Miller et al., 2013a).

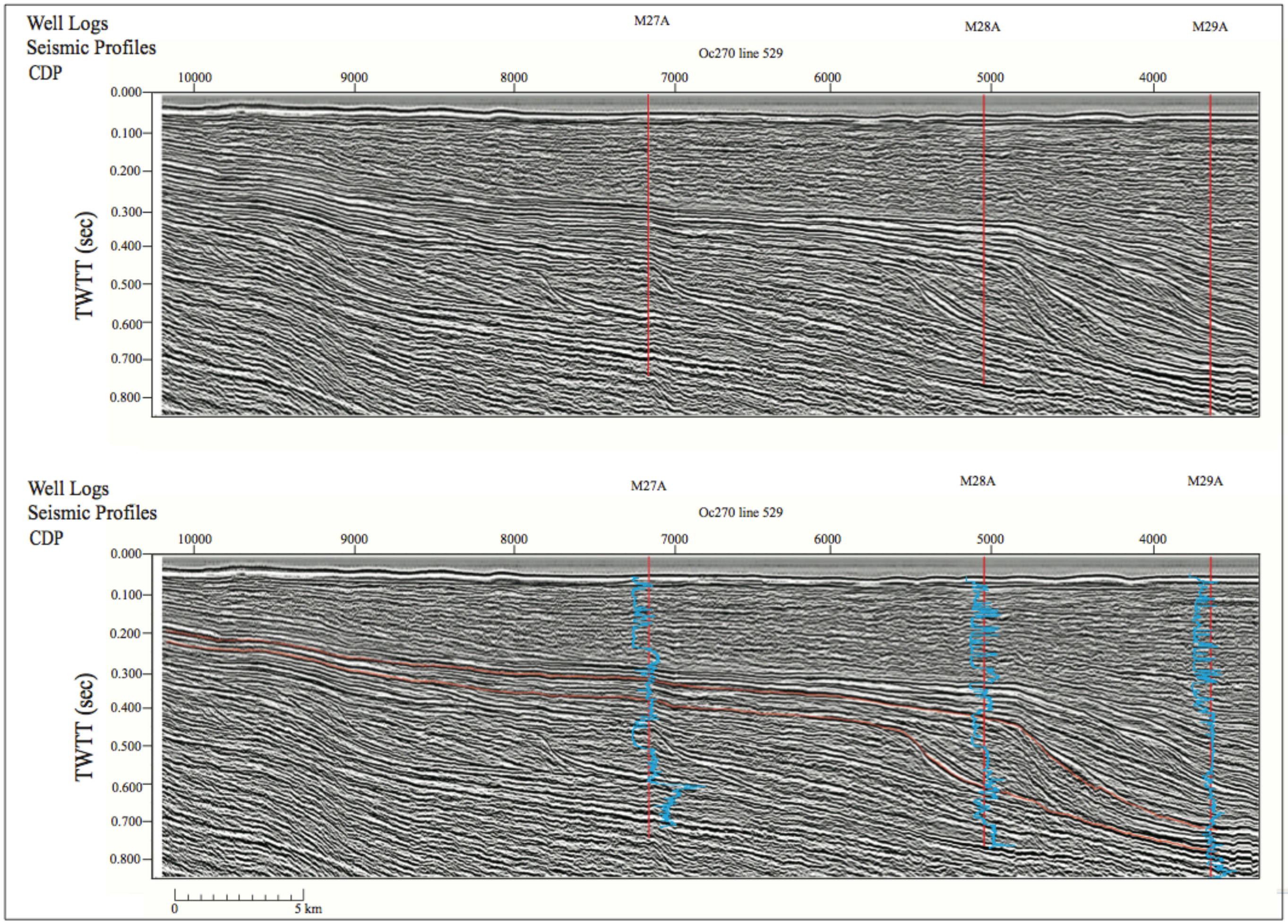

Figure 20: The red colored reflections show offshore equivalents of top and basal sequence boundaries of composite Kw2a sequence traced from CH0698 38 seismic profile to Oc270 529 seismic profile. (A closer view of Oc270 529 part of fig. 19)

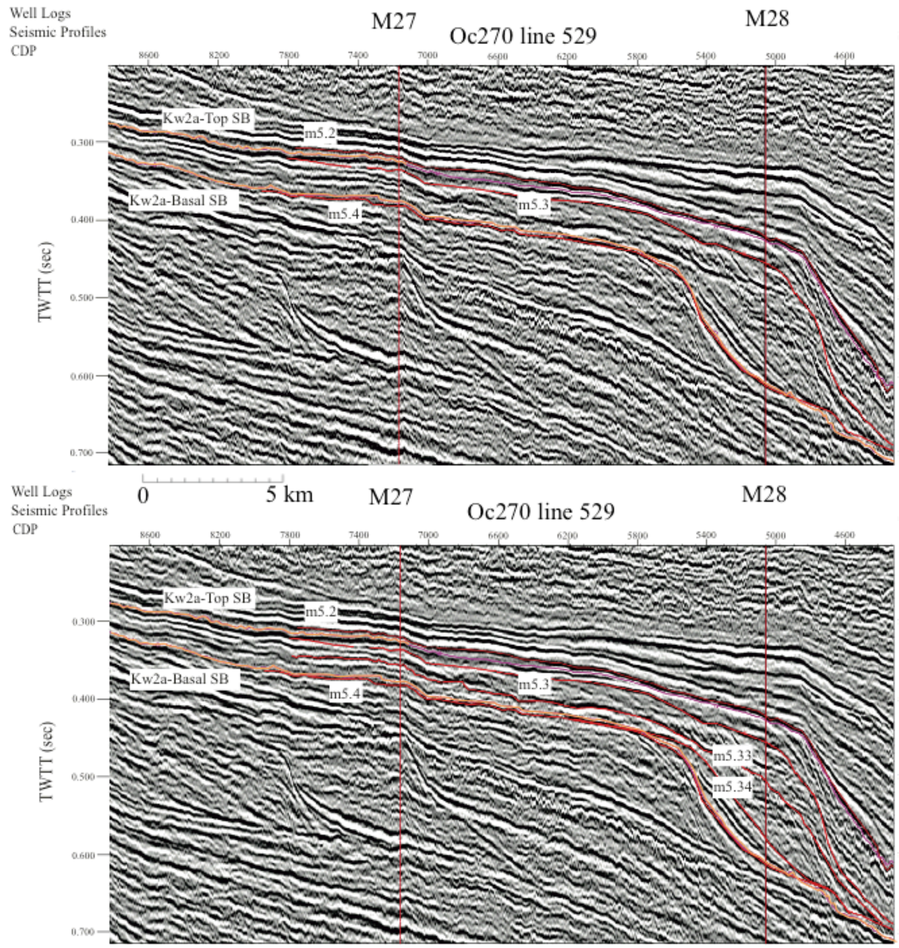

Figure 21: The orange reflections show top and base of Kw2a composite sequence. Red colored reflections are gathered from Miller et al. (2013a). Upper sequence boundary of Kw2a seems to merge with m5.3 reflection at the landward side of M27, where seismic ambiguity occurs due to truncated m5.3 reflectionand continuonus tracing might lead to m5.2 reflection.

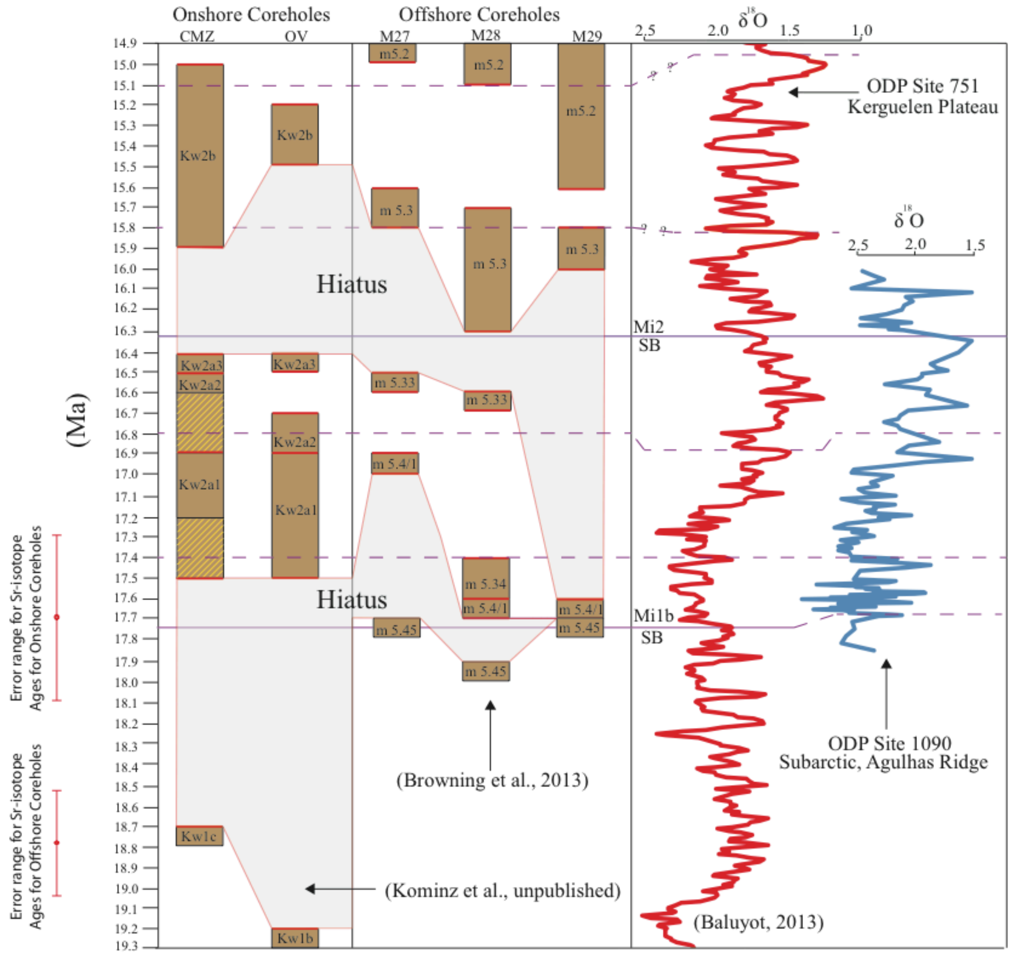

Figure 22: Comparison of Expedition 313 coreholes (M27, M28, and M29) ages Browning et al. (2013), Cape May Zoo and Ocean View coreholes Sr-isotope age data Kominz et al. (unpublished) and $\delta^{18}O$ data comparison with Mi events. Mi1b and Mi2 events mark the sequence boundaries for onshore Kw2a and offshore m5.4 composite sequences.

8 Tables

Well Logs	Atlantic City	Ocean View	Cape May Zoo	Cape May	ACOW-1	ACOW-2	Sea Isle City	Strathmere	AMCOR-6011
Core and well log based thicknesses									
Upper Sequence Boundary (m)	156	141	155	187	182	216	126	148	138
Lower Seuence Boundary (m)	203	195	192	216	230	268	186	207	168
Thickness (m)	47	54	37	29	48	52	60	59	30
After application of T-D chart seismic thickness									
Upper Seismic Reflection (m)	156	140	154	191	180	216	165	148	138
Lower Seismic Reflection (m)	206	195	194	217	232	270	221	206	168
Thickness (m)	50	55	40	26	52	54	56	58	30
Well Log Projection Information									
Distance to projected seismic line (m)	770	5800	10080	4200	245	25	2500	2135	25
Displayed seismic line	ch027	ch042	ch042	ch042	ch038	ch0016	ch042	ch042	ch016
Estimated projection in meters from ch005and ch009	4.8	36.1	62.8	26.2	1.5	0.2	15.6	13.3	0.2
Applied projection in meters to seismic profiles	-	24	55	32	-	-	4	16	-

Table 1: The original well log thicknesses are compared with the thicknesses of sequences after application of T-D chart and displayed on seismic profiles. This table also provides minimum distance between well log and nearest seismic profile and vertical dipline gradient for individual wells.

ch0698 Seismic Profile 9	TWT of First Point (sec)	TWT of Last Point (sec)	Lateral Traced Distance (m)	Thickness Difference (m)	Estimated Gradient (m)
TWTT of Upper Seismic Reflection (Red) (sec)	0.203	0.244	5900	0	36.39
TWTT of Lower Seismic Reflection (Red) (sec)	0.260	0.301	5900	-	36.39
TWTT Difference (sec)	0.057	0.057		-	-
Average Gradient (m)	-	-	-	-	36.39
	-	-	-	-	-
ch0698 Seismic Profile 5	TWT of First Point (sec)	TWT of Last Point (sec)	Traced Lateral Distance (m)	Thickness Difference (m)	Estimated Gradient (m)
TWTT of Upper Seismic Reflection (Green) (sec)	0.220	0.299	10800	5	70.11
TWTT of Lower Seismic Reflection (Green) (sec)	0.264	0.338	10800	-	65.68
TWTT Difference (sec)	0.044	0.039	-	-	-
Estimeted Average Gradient (m)	-	-	-	-	67.89
Overall Estimated Average Gradient (m)	-	-	10000	2.5	62.27

Table 2: The gradient and thickening estimation, are shown on this table with providing TWTT (two way travel time) and lateral traced distances individually on CH0698 5 and 9 seismic profiles. Overall average is estimated by taking mean of the two different estimations.

Depth (ft)	Sample Weight (g)	Sample Weight x Splitting Ratio (g)	Number of Planktonic Foraminifera	Planktonic # / Total Foraminifera (%)	Number of Benthic Foraminifera	Benthic # / (Sample Weight x Splitting Ratio) g
515.90	5.74	5.74	7.00	3.15	222.00	38.68
521.00	1.98	1.98	0.00	0.00	0.00	0.00
526.00	12.00	12.00	0.00	0.00	2.00	0.17
531.00	22.46	22.46	0.00	0.00	3.00	0.13
536.50	18.36	18.36	0.00	0.00	0.00	0.00
541.00	18.60	18.60	0.00	0.00	0.00	0.00
546.00	21.18	21.18	2.00	40.00	5.00	0.24
551.00	1.78	1.78	6.00	6.59	91.00	51.12
556.00	5.74	5.74	3.00	1.17	257.00	44.77
561.00	13.00	13.00	0.00	0.00	73.00	5.62
566.00	0.52	0.52	0.00	0.00	9.00	17.31
571.00	0.56	0.56	2.00	15.38	13.00	23.21
576.00	5.02	5.02	13.00	5.94	219.00	43.63
581.00	0.30	0.30	1.00	4.76	21.00	70.00
586.00	1.22	1.22	0.00	0.00	0.00	0.00
591.00	3.12	3.12	0.00	0.00	0.00	0.00
601.00	5.96	5.96	1.00	9.09	11.00	1.85
606.00	15.88	15.88	0.00	0.00	0.00	0.00
611.00	1.36	1.36	0.00	0.00	15.00	11.03
616.00	3.32	3.32	0.00	0.00	1.00	0.30
620.30	10.28	10.28	0.00	0.00	0.00	0.00
621.00	2.42	2.42	3.00	4.17	72.00	29.75
626.00	21.48	10.74	15.00	4.31	348.00	32.40
626.90	45.14	45.14	6.00	2.45	245.00	5.43
627.60	11.06	11.06	0.00	0.00	6.00	0.54
630.20	-	-	0.00	0.00	0.00	-

Table 3: Sample data of CMZ corehole composite Kw2a sequence and benthic and planktonic foramifera numarical values are provided.

Depth (ft)	First Dominant Biofacies	Second Dominant Biofacies	Third Dominant Biofacies	Fourth Dominant Biofacies	Fifth Dominant Biofacies
516.00	*Hanzawaia* spp. (107, 48.20%)	*Pseudononion* spp. (97, 43.69%)	*Textularia* spp. (4, 1.80%)	*Lagena* spp. (3, 1.35%)	*Bulimina* spp. (2, 0.90%)
521.00	–	–	–	–	–
526.00	*Hanzawaia* spp. (1, 50.00%)	*B. elegantissima* (1, 50%)	–	–	–
531.00	*Hanzawaia* spp. (1, 16.67%)	*Textularia* spp. (4, 66.66%)	Cracked specimen (1, 16.67%)	–	–
537.00	–	–	–	–	–
541.00	–	–	–	–	–
546.00	*B. elegantissima* (3, 60%)	*Bulimina* spp. (1, 20.00%)	*Bolivina* spp. (1, 20.00%)	–	–
551.00	*Hanzawaia* spp. (34, 37.36%)	*Bulimina* spp. (23, 25.27%)	*Pseudononion* spp. (8, 8.79%)	*Pseudopolymorphina* spp. (8.79%)	*Cibicides* spp. (8, 8.79%)
556.00	*Hanzawaia* spp. (166, 64.59%)	*Pseudononion* spp. (20, 7.78%)	*Bulimina* spp. (15, 5.84%)	*Cibicides* spp. (11, 4.28%)	*Bolivina* spp. (10, 3.89)
561.00	*B. elegantissima* (31, 42.47%)	*Bolivina* spp. (19, 26.03%)	*Hanzawaia* spp. (17, 23.29%)	*Pseudononion* spp. (2, 2.74%)	*Bulimina* spp. (1, 1.37%)
566.00	*Pseudononion* spp. (9, 100.00%)	–	–	–	–
571.00	*Pseudononion* spp. (9, 69.23%)	*Bulimina* spp. spp. (4, 30.77%)	–	–	–
576.00	*Pseudononion* spp. (126, 57.53%)	*B. elegantissima* (42, 19.18%)	*Bulimina* spp. (12, 5.48%)	*Bolivina* spp. (10, 4.57%)	*Uvigerina* spp. (7, 3.20%)
581.00	*Uvigerina* spp. (11, 52.38%)	*Pseudononion* spp. (10, 47.62%)	–	–	–
586.00	–	–	–	–	–
591.00	–	–	–	–	–
601.00	*Pseudononion* spp. (4, 36.36%)	*Hanzawaia* spp. (4, 36.36%)	*Bulimina* spp. (1, 9.09%)	*B. elegantissima* (1, 9.09%)	*Uvigerina* spp. (1, 9.09%)
606.00	–	–	–	–	–
611.00	*Pseudononion* spp. (11, 73.33%)	*Bulimina* spp. spp. (2, 13.33%)	*Hanzawaia* spp. (1, 6.67%)	*Bulimina* spp. (1, 6.67%)	–
616.00	*Hanzawaia* spp. (1, 100.00%)	–	–	–	–
620.00	–	–	–	–	–
621.00	*Pseudononion* spp. (32, 44.44%)	*Hanzawaia* spp. (22, 30.56%)	*Bulimina* spp. (8, 11.11%)	*Uvigerina* spp. (5, 6.94%)	*Bolivina* spp. (2, 2.78%)
626.00	*Hanzawaia* spp. (257, 73.85%)	*Textularia* spp. (38, 10.92%)	*Uvigerina* spp. (17, 4.89%)	*Pseudononion* spp. (13, 3.74%)	*Bulimina* spp. (5, 1.44%)
626.90	*Hanzawaia* spp. (214, 87.35%)	*Spiroplectammina carinata* (19, 7.76%)	*Pseudononion* spp. (6, 2.45%)	*Lenticulina* spp. (5, 2.04%)	*Uvigerina spp.* (1, 0.41%)
627.60	*Hanzawaia* spp. (5, 83.33%)	*Textularia* spp. (1, 16.67%)	–	–	–
630.20	–	–	–	–	–

Table 4: CMZ corehole first five predominant benthic foraminiferal biofacies are provided with numerical values and relative precentages for each sample.

Depths (ft)	Sample Weigh (g)	Sample Weight x Splitting Ratio (g)	Number of Planktonic Foraminifera	Planktonic # / Total Foraminifera (%)	Number of Benthic Foraminifera	Benthic # / (Sample Weight x Spliting Ratio) (g)
465.20	40.10	2.51	0	0.00	0	0.00
466.00	44.10	44.10	0	0.00	0	0.00
471.00	41.96	41.96	0	0.00	0	0.00
476.00	40.32	40.32	0	0.00	0	0.00
480.90	28.22	28.22	0	0.00	0	0.00
490.00	28.00	28.00	1	0.69	143	5.11
496.00	10.70	10.70	0	0.00	30	2.80
500.00	11.60	11.60	5	3.07	158	13.62
502.20	10.12	10.12	0	0.00	1	0.10
505.00	36.70	36.70	0	0.00	1	0.03
510.00	38.70	38.70	0	0.00	2	0.05
515.00	39.80	39.80	2	14.29	12	0.30
521.00	37.40	37.40	0	0.00	0	0.00
526.10	33.40	33.40	0	0.00	0	0.00
530.80	1.40	1.40	0	0.00	244	174.29
536.00	20.20	10.10	3	0.97	306	30.30
541.00	10.80	10.80	0	0.00	190	17.59
546.00	14.40	5.40	2	0.54	366	67.78
551.00	5.00	5.00	0	0.00	0	0.00
561.00	0.60	0.60	0	0.00	1	1.67
566.00	1.00	1.00	0	0.00	8	8.00
571.00	2.00	2.00	0	0.00	3	1.50
576.00	1.50	1.50	0	0.00	4	2.67
581.00	0.50	0.50	0	0.00	3	6.00
586.00	1.90	1.90	3	6.67	42	22.11
591.00	0.40	0.40	0	0.00	9	22.50
596.00	1.30	1.30	3	2.24	131	100.77
601.00	2.50	0.31	28	5.42	489	1564.80
606.00	0.30	0.30	1	3.33	29	96.67
611.00	0.40	0.10	0	0.00	475	4750.00
616.00	0.30	0.30	0	0.00	2	6.67
621.00	8.70	8.70	6	2.51	233	26.78
626.00	10.18	10.18	16	3.84	401	39.39
628.00	10.48	10.48	0	0.00	98	9.35
631.00	23.50	5.88	1	0.30	332	56.51
636.40	32.90	32.90	0	0.00	0	0.00

Table 5: Sample data of OV corehole composite Kw2a sequence, benthic and planktonic foramifera numarical values are provided.

Depth (ft)	First Dominant Biofacies	Second Dominant Biofacies	Third Dominant Biofacies	Fourth Dominant Biofacies	Fifth Dominant Biofacies
465.20	–	–	–	–	–
466.00	–	–	–	–	–
471.00	–	–	–	–	–
476.00	–	–	–	–	–
480.90	–	–	–	–	–
490.00	*Bulimina* spp. (4, 40%)	*Hanzawaia* spp. (3, 30%)	*Pseudononion* spp. (2, 20%)	*Pseudopolymorhina* rutila (1, 10%)	–
496.00	*Pseudononion* spp. (16, 53.33%)	*Hanzawaia* spp. (8, 26.67%)	*Bulimina* spp. (5, 16.67%)	*S. carinata* (1, 3.33%)	–
500.00	*Hanzawaia* spp. (65, 41.14%)	*S. carinata* (50, 31.65%)	*Pseudononion* spp. (31, 19.62%)	*Pseudopolymorphina rutila* (3, 1.90%)	*Bolivina* spp. (2, 1.27%)
502.20	*Spiroplectammina carinata* (1, 100%)	–	–	–	–
505.00	*Hanzawaia* spp. (1, 100%)	–	–	–	–
510.00	Cracked specimens (2,100%)	–	–	–	–
515.00	*Lenticulina* spp. (4, 33.33%)	*Elphidium* spp. (3, 25%)	*Hanzawaia* spp. (1, 8.33)	*Pseudononion* spp. (1, 8.33%)	Cracked specimens (3, 25%)
521.00	–	–	–	–	–
526.10	–	–	–	–	–
530.80	*B. elegantissima* (124, 50.82%)	*Bolivina* spp. (58, 23.77%)	*Pseudononion* spp. (42, 17.21%)	*Bulimina* spp. (5, 2.05%)	*Elphidium* spp. (4, 1.64%)
536.00	*B. elegantissima* (104, 39.99%)	*Pseudononion* spp. (76, 24.84%)	*Hanzawaia* spp. (51, 16.67)	*Elphidium* spp. (34, 11.11%)	*Bolivina* spp. (13, 4.25%)
541.00	*Hanzawaia* spp. (67, 35.26%)	*Elphidium* spp. (49, 25.79%)	*Pseudononion* spp. (43, 22.63%)	*Bulimina* spp. (9, 4.74%)	*B. elegantissima* (3, 1.58%)
546.00	*Hanzawaia* spp. (180, 49.18%)	*Pseudononion* spp. (143, 39.07%)	*Uvigerina* spp. (19, 5.19%)	*Elphidium* spp. (16, 4.37%)	*Bulimina* spp. (3, 0.82%)
551.00	–	–	–	–	–
561.00	*B. elegantissima* (1, 100%)	–	–	–	–
566.00	*Pseudononion* spp. (3, 37.50%)	*B. elegantissima* (2, 25.00%)	*Bolivina* spp. (2, 25.00%)	*Uvigerina* ssp. (1 ,12.50%)	–
571.00	*Pseudononion* spp. (2, 66.77%)	*Hanzawaia* spp. (1, 33.33%)	–	–	–
576.00	*Pseudononion* spp. (3, 75.00%)	*Uvigerina* ssp. (1 ,25.00%)	–	–	–
581.00	*Pseudononion* spp. (4, 100.00%)	–	–	–	–
586.00	*Pseudononion* spp. (36, 85.71%)	*Hanzawaia* spp. (3, 7.14%)	*Uvigerina* ssp. (1 ,2.38%)	Cracked specimens (2,4.76%)	–
591.00	*Pseudononion* spp. (6, 66.67%)	*Bulimina* spp. (1, 11.11%)	*Elphidium* spp. (1, 11.11%)	*Uvigerina* spp. (1, 11.11%)	–
596.00	*Pseudononion* spp. (51, 38.93%)	*Uvigerina* spp. (47, 35.88%)	*Hanzawaia* spp. (27, 20.61%)	*Bulimina* spp. (5, 3.82%)	*Lenticulina* spp. (1, 0.76%)
601.00	*Uvigerina* spp. (229, 46.83%)	*Pseudononion* spp. (130, 26.58%)	*Hanzawaia* spp. (103, 21.06%)	*Lenticulina* spp. (21, 4.29%)	*Bulimina* spp. (2, 0.41%)
606.00	*Pseudononion* spp. (17, 58.62%)	*Hanzawaia* spp. (6, 20.69%)	*Uvigerina* spp. (4, 13.79%)	*Lagena* spp. (2, 6.90%)	
611.00	*Hanzawaia* spp. (324, 68.21%)	*Pseudononion* spp. (51, 10.74%)	*Lenticulina* spp. (37, 7.79%)	*Uvigerina* spp. (29, 6.11%)	*Bolivina* spp. (27, 5.68%)
616.00	*Hanzawaia* spp. (1, 50.00%)	*Lenticulina* spp. (1, 50.00%)	–	–	–
621.00	*Hanzawaia* spp. (111, 47.64%)	*Lenticulina* spp. (43, 18.45%)	*Uvigerina* spp. (30, 12.88%)	*Pseudononion* spp. (18, 7.73%)	*Bulimina* spp. (7, 3.00%)
626.00	*Pseudononion* spp. (283, 70.57%)	*Hanzawaia* spp. (75, 18.70%)	*Bulimina* spp. (20, 4.99%)	*B. elegantissima* (7, 1.75%)	*Bolivina* spp. (4, 1.00%)
628.00	*Hanzawaia* spp. (37, 37.75%)	*Pseudononion* spp. (28, 28.57%)	*Uvigerina* spp. (19, 19.38%)	*Bulimina* spp. (9, 9.18%)	*Lenticulina* spp. (3, 3.06%)
631.00	*Pseudononion* spp. (128, 38.55%)	*Hanzawaia* spp. (98, 29.52%)	*Uvigerina* spp. (27, 8.13%)	*Bulimina* spp. (18, 5.42%)	*Lenticulina* spp. (11, 3.31%)
636.40	–	–	–	–	–

Table 6: OV corehole first five predominant benthic foraminiferal biofacies are provided with numerical values and relative precentages for each sample